Fall 2022

Experimental Investigations of Yarn Pull-Out Behavior in Kevlar®: Influence of Applied Metallic Coatings and Effect of Dynamic Loading

Julie Ann Roark

EXPERIMENTAL INVESTIGATIONS OF YARN PULL-OUT BEHAVIOR IN KEVLAR®: INFLUENCE OF APPLIED METALLIC COATINGS AND EFFECT OF DYNAMIC LOADING

by

Julie Ann Roark

Bachelor of Science
University of South Carolina, 2020

Submitted in Partial Fulfillment of the Requirements

For the Degree of Master of Science in

Mechanical Engineering

College of Engineering and Computing

University of South Carolina

2022

Accepted by:

Subramani Sockalingam, Director of Thesis

Daniel O'Brien, Reader

Cheryl L. Addy, Interim Vice Provost and Dean of the Graduate School

ACKNOWLEDGEMENTS

Researching funding for the author was sponsored by the US Army Contracting Command-APG, Natick Contracting Division, Natick, MA and by Directed Vapor Technologies International, INC. Army Research Laboratory at Aberdeen Proving Ground, Maryland and McNair Aerospace Center at the University of South Carolina, SC provided equipment, facilities, and support training for experimental testing. The opinions, findings, conclusions, or recommendations expressed in this document are those of the author(s) and do not necessarily reflect the views of the US Army Contracting Command-APG, Natick Contracting Division, Natick, MA or Direct Vapor Technologies International, Inc. Kevlar® S706 woven fabric used in this work was provided by ARL/DuPont and is gratefully acknowledged. The United States government is authorized to reproduce and distribute reprints for government purposes notwithstanding any copyright notation herein.

The author would like to acknowledge Dr. Daniel O'Brien and Mr. Paul Moy of Army Research Laboratory at Aberdeen Proving Ground, Maryland for their support with both administrative and technical concerns throughout the project. Furthermore, the author would like to acknowledge Mr. Frank Thomas for the advanced modeling technical support, Dr. Scott Crittenden for the assistance with single fiber imaging on the Atomic-Force Microscope, and Dr. Subramani Sockalingam for his guidance and persistence in the development of this thesis.

ABSTRACT

Flexible woven Kevlar® textile fabrics are widely used in protective armor applications. Yarn pull-out, comprised of yarn uncrimping (i.e., straightening) and yarn translation, is a major energy absorption mechanism during ballistic impact onto these fabrics, especially for impact velocities below the ballistic limit. Yarn pull-out is influenced by various parameters including inter-yarn friction, pull-out distance, pull-out velocity, transverse pre-tension, fiber diameter, fabric architecture, fabric waviness, fabric count and yarn modulus.

The first part of this thesis investigates yarn pull-out behavior of commercially available Kevlar® KM2+ individual yarns coated with metallic layers (copper, aluminum, aluminum nitride, silver) via a directed vapor deposition process. The uncoated control and metal-coated Kevlar® yarns are hand-woven into fabric swatches for quasi-static pull-out experiments. To perform these experiments, a yarn pull-out fixture is custom-designed and fabricated to apply transverse pre-tension to the fabric. Three levels of transverse pre-tensions are studied at 100 N, 200 N, and 400 N. Both peak pull-out force and energy absorption during the pull-out process is found to increase with increase in transverse pre-tension. All the metal-coated groups showed an approximately 200% increase in peak pull-out force and a 20% reduction in tenacity compared to uncoated control. Furthermore, all the metal-coated groups showed an increase in energy absorption, with aluminum-coated yarns showing the highest increase of 230% compared to control. These results suggest enhanced frictional interactions during yarn pull-out in

metal-coated yarns compared to uncoated control as evidence by the frictional calculations.

The second part of this thesis investigates the yarn pull-out response of dynamic loading on Kevlar® K2+ woven specimens. A custom testing woven fabric fixture and single yarn grip fixture was designed and fabricated. The dynamic loading rates are studied at 15 m/s, 20 m/s, and 25 m/s. Peak force and energy absorption increased as the displacement rate increased for both tested L=27 mm and L=5 mm specimens. In the L=27 mm dynamic tested specimens, there was 33% increase in peak force and approximately 110% increase in energy absorbed with an increase in displacement rate. Quasi-static L=27 mm compared to dynamic L=27 mm specimens there was 528% increase in peak force, and 600% increase in energy absorbed. Studying dynamic experimental loading rates L=5 mm specimens show a 50% increase with an increase from 15 m/s to 20 m/s, but a slight decrease in peak force once reaching highest tested displacement rate. L=5 mm dynamic tested specimens energy absorption values show approximately a 130% increase with an increase in displacement rate. For Quasi-static to dynamic loading rates L=5 mm specimens presented a 900% increase from 1 mm/s to 20 m/s with a slight percentage decrease once reaching 25 m/s. The energy absorption from quasi-static to dynamic loading rates in L=5 mm experiments display a 700% increase in energy absorbed results of S706 fabric. All dynamic loading test showed higher peak forces and energy absorption values than quasi-static experiments. The results insinuate higher peak forces and energy absorption results which can be directly correlated to improved ballistic performance.

TABLE OF CONTENTS

LIST OF TABLES

LIST OF FIGURES

CHAPTER 1

INTRODUCTION

1.1 BACKGROUND AND MOTIVATION

Kevlar was invented in the 1965 to achieve performance goals of casualty reduction testing for the Department of Defense with the exceptional properties of strength and stiffness. Kevlar is being integrated into the everyday use for the United States military. The material is found in helmets and vests due to the enhanced bullet and fragmentation resistance while delivering comfort and breathability in all climate conditions. The innovation of Kevlar has produced properties such as thermal stability, water repellant, chemical stability, and resistance to petroleum products which has allowed Kevlar to become an indispensable asset to military personnel.

Kevlar is a heat-resistance para-aramid synthetic fiber with a chemical compound of poly-para-phenylene terephthalamide [29]. At the core Kevlar is extremely light weight, yet strong synthetic polymer that is weaved into a yarn material that is five times stronger than a steel wire which is why it is highly desirable for many applications compared to conventional materials. Once manufactured into the fiber form, it is then made into a thread that can be woven into a fabric and used for numerous applications. A major characteristic of Kevlar it that it is strong as it is by itself, but when paired with other materials it can become even stronger making the study of Kevlar and other materials a desirable goal for research and industry functions [30]. Theoretically from the combined

studies of modified Kevlar, the improved characteristics can produce a combat shirt integrator for garment level demonstrations. Experimental testing has made great efforts in understanding the mechanisms of Kevlar material, but improvements are needed to quantify the behavior of metallic coated fibers and high loading rates on woven Kevlar fabrics.

Despite the high strength and stiffness characteristics, further research of weight reductions, energy dissipation, and advanced ballistic performance are needed in Kevlar® material. The first objective is to modify the surface properties of Kevlar fibers/yarns to enhance the energy dissipation mechanics present in Kevlar fabrics during ballistic impact events. This approach will alter the properties of Kevlar through continuous fiber coating systems that will apply metallic coatings to ballistic fibers. Hypothetically, these metallic coatings will increase the frictional coefficients that have a proven correlation to improving ballistic performance. The idea of applying metallic coatings to the bare traditional Kevlar is designed to modify the work required to compress Kevlar fibers during impact and to limit fiber damage that can reduce its tensile strength. Traditional approaches consist of applications of shear thickening fluids [9], silica nanoparticles [10,11], and carbon nanotubes [7] Previously, surface treatments are originally applied to fabrics and not individual yarns due to the potential increase of damage on the yarns during the weaving process that would result in a tensile strength reduction. The downfall to coating fabrics the area inside cross-over yarns may not be coated or effectively coated. Metal-based treatments on individual Kevlar® yarns are unstudied. The second goal is to test Kevlar woven fabrics under dynamic loading to establish the dynamic behavior of Kevlar. The technique used to achieve the high loading rate was a Split

Hopkinson Pressure Bar. Previously studies of dynamic loading conditions on Kevlar® were conducted at loading rates of 1.37 m/s using a pendulum impact test setup [23]. The second objective is to test the same Kevlar® S706 fabrics at loading rates of 15 m/s, 20 m/s, and 25 m/s. To understand the performance of a bullet proof vest requires adequate knowledge about the characteristics of woven fabrics. Prior literature results are a model to understanding the response of Kevlar® fabrics under quasi-static and dynamic testing conditions. Both approaches pose new challenges to the experimental design regarding testing instrumentation, data recorded, and necessary fixtures that will be required for testing. The experiments will be conducted on a smaller scale to characterize and quantify the response that can be applied to larger scale applications. In efforts to expand the knowledge of Kevlar material, this thesis presents a two experimental processes of testing Kevlar woven fabrics with applied metallic coatings and Kevlar fabrics tested under diverse loading rates with comparisons made to results from existing testing methods.

1.2 RESEARCH OBJECTIVES

The main objective of this research is to investigate yarn-pull out behavior of individual metallic coated Kevlar® KM2+ yarns, and the pull-out response of dynamic loading on woven Kevlar® KM2+ fabrics. To fulfill this task, several steps are required. First, the existing literature must be critically studied to understand the experimental data and characteristics of Kevlar® KM2+. Next, an experimental procedure and testing parameters for studying the added metallic coatings response and various dynamic loadings must be drafted. The details of the addition of transverse pre-tension to the designed quasi-static experiment must be determined, and the necessary components to test the Kevlar woven fabrics with specified dimensions under dynamic loading must be

determined. Finally, all information must be understood and applied to successfully comprehend the capabilities of metallic coated Kevlar® KM2+ yarns and Kevlar® KM2+ tested at high ballistic performance rates.

1.3 THESIS OUTLINE

This thesis will satisfy these objectives as follows:

Chapter 2 presents current state of the art on yarn pullout response

Chapter 3 discusses the experimental design and methodology for quantifying quasi-static results of uncoated and metallic coated Kevlar

Chapter 4 details the experimental design and methodology for quantifying dynamic results of uncoated and metallic coated Kevlar

Chapter 5 concludes the thesis with extensive explanation of methodology and results

CHAPTER 2

LITERATURE REVIEW

This literature review chapter examines the existing knowledge of literature, past as well as current, and relates the knowledge to the performance characteristics of ballistic impact of Kevlar material and two new approaches to increase ballistic performance presented.

2.1 QUASI STATIC YARN PULL-OUT EXPERIMENTS

Flexible woven textile fabrics utilizing Kevlar® fibers are widely used in protective armor applications [1]. During impact, longitudinal and transverse waves develop and propagate in the principal yarns in a fabric that are in direct contact with the projectile. The longitudinal waves in the primary yarns drive the longitudinal waves in the secondary yarns, thus providing an effective transverse impact on the secondary yarns [2]. The yarn material behind the longitudinal wave front moves inward towards the impact point resulting in yarn pullout over the crossover points. Yarn pull-out without premature yarn failure [3] is shown to have a positive correlation to the ballistic impact performance of aramid fabrics [4] due to increased yarn pull-out force and energy dissipation during the pull-out process. Yarn pull-out is influenced by various parameters including inter-yarn friction, pull-out distance, pull-out rate, pull pattern, transverse pre-tension, fiber diameter, fabric architecture, fabric waviness, fabric count and yarn modulus [4–6].

Inter-yarn friction during yarn pull-out is an important energy dissipating mechanism during ballistic impact onto woven fabrics. Increased frictional interactions between the yarns have been shown both experimentally [7] and numerically [8] to improve the ballistic performance of Kevlar fabrics. Previous studies have shown that impact performance can be improved by impregnating the fabrics with shear thickening fluid [9], silica nanoparticles [10,11] and carbon nanotubes [7]. A 230% increase in quasi-static yarn pull-out force with tensile strength statistically similar to the neat yarn and a 50% increase in the ballistic limit is reported in [7] for Kevlar® 129 fabrics treated with multi-walled carbon nanotubes. Also, in these studies, surface treatments are typically applied to the fabrics rather than to the individual yarns, because weaving of the treated yarns into a fabric may introduce additional damage resulting in tensile strength reduction. However, the tradeoff is since the treatment is applied on fabrics, yarn surfaces inside the crossover points may not be as effectively coated. In all these studies, a polymer-based surface treatment is typically employed to treat the fabrics. Whereas metal-based treatments via vapor deposition techniques for increasing inter-yarn friction is largely unexplored.

Directed vapor deposition (DVD) process [12] can apply well adhered, inorganic layers onto long lengths of continuous synthetic fibers. The DVD approach provides the technical basis for a flexible, high quality coating process capable of atomistically depositing dense, compositionally controlled coatings onto line-of-sight and non-line-of-sight regions of substrates. Unlike other physical vapor deposition approaches, DVD is specifically designed to enable the transport of vapor atoms from a source to a substrate. To achieve this, DVD technology utilizes a supersonic gas jet to direct and transport a

thermally evaporated vapor cloud onto a component. Typical operating pressures are in the 1 to 50 Pa range. In this processing regime, collisions between the vapor atoms and the gas jet create a mechanism for controlling vapor transport. This enables highly efficient, high-rate deposition (>10 m/min), non-line-of-sight deposition, and the ability to deposit metals, complex alloys, ceramic layers (including ultra-hard materials) and nano-laminate composites onto complex substrates. The combination of these attributes provides a cost-effective, continuous deposition approach for applying functional layers onto fibers/yarns in a high throughput manner.

While many materials have a higher coefficient of friction than Kevlar® (neat Kevlar® 129 has a relatively low coefficient of static friction μ_s of ~0.22 [7]), it is of interest to note that metal-on-metal sliding of simple metals such as Al, Ni, Au, Sn and Cu can have significantly higher μ_s values (μ_s (Al-Al) = 1.0-1.3; μ_s (Cu-Cu) = 1.0; μ_s (Au-Au) = 2.0; μ_s (Ni-Ni) = 0.7-1.1; μ_s (Sn-Sn) = 1.4) [13–16]. It should also be noted that such friction values are a function of the loads applied. The low density of Al makes thin (nanoscale) layers of well adhered Al of interest for enhancing ballistic performance via DVD, although the role of oxide scale which forms on the Al surface in ambient environments on its friction coefficient under dynamic loading conditions is unclear. Other advanced layers also appear feasible via DVD. These include nano-laminates (such as Al/AlN) that may enhance energy dissipation during transverse fiber compression (this compression can be substantial during impact events) [17] through the creation of a high surface area of crack propagation along the multiple Al/AlN interfaces.

2.2 DYNAMIC YARN PULL-OUT EXPERIMENTS

2.2.1 Characteristics of Kevlar tested in dynamic loading conditions

Flexible woven Kevlar® textile fabrics are widely used in protective armor applications [1]. Yarn pull-out, comprised of yarn uncrimping (i.e., straightening) and yarn translation, is a major energy absorption mechanism during ballistic impact onto these fabrics [2], especially for impact velocities below the ballistic limit. Yarn pull-out is influenced by various parameters including inter-yarn friction, pull-out distance, pull-out velocity, transverse pre-tension, fiber diameter, fabric architecture, fabric waviness, fabric count and yarn modulus [3–5]. At relatively low impact velocities (< 300 m/s), the expected yarn pull-out velocity during impact is around 15 m/s [2].

While several studies report quasi-static yarn pull-out response of Kevlar® fabrics, typically in the range of 50 mm/min to 500 mm/min [3–5], studies concerning dynamic yarn pull-out are very limited. Guo et al. [6] performed dynamic out-of-plane yarn pull-out testing at ~1 m/s in a pendulum impact setup. They observed increases in peak pull-out force, displacement at peak force and uncrimping energy with increase in loading rate from 1 mm/s to 1 m/s. Inter-yarn friction during yarn pull-out is an important energy dissipating mechanism during ballistic impact onto woven fabrics. Increased frictional interactions between the yarns have been shown both experimentally [7] and numerically [8] to improve the ballistic performance of Kevlar fabrics. Previous studies have shown that impact performance can be improved by impregnating the fabrics with shear thickening fluid [9], silica nanoparticles [10,11] and carbon nanotubes [7]. Also, in these studies, surface treatments are typically applied to the fabrics rather than to the individual yarns, because weaving of the treated yarns into a fabric may introduce additional damage resulting in tensile strength reduction. However, the tradeoff is since the treatment is applied on fabrics, yarn surfaces inside the crossover points may not be

as effectively coated. In all these studies, a polymer-based surface treatment is typically employed to treat the fabrics. Whereas metal-based treatments via vapor deposition techniques for increasing inter-yarn friction is largely unexplored.

For the first time, this paper proposes an experimental method for dynamic yarn pull-out testing of flexible textile fabrics at pull-out velocities in the range of 15 m/s to 25 m/s. In this method, a modified tensile Hopkinson bar setup with a custom-designed yarn pull-out fixture along with high-speed cameras is utilized. This setup and a previously developed quasi-static yarn pull-out fixture are employed to investigate the dynamic and quasi-static yarn pull-out response of commercially available Kevlar® S706 plain-woven fabrics.

2.2.2 Properties of Kevlar S706 Fabric

The Kevlar fabric used in this study is Kevlar S706 woven fabric. Kevlar S706 is a balanced plain weave fabric with an areal density of 180 g/m^2 and contains 600 denier Kevlar KM2+ yarns with a yarn span of 0.747 mm. The fabric material test was in an “as is” condition manufactured and provided by Dupont and the Army Research Lab (ARL) located at Aberdeen Proving Grounds, MD, USA. Figure 4.2 displays the image of the Kevlar S706 material that has been properly prepared for an experimental test.

2.3 SUMMARY

Modified Kevlar material and high-performance rates are important research objective for predicating the efficiency of ballistic armor systems. Initial work has been understanding the characteristics of metallic coated yarns versus uncoated yarns. The initial work has also included the understanding of quasi-static results with no applied transverse pre-tension under loading rates of 1 mm/s. The beginning of both approaches included the

comprehension of existing experimental methodology that provides a foundation for the future testing. Later work has moved to quantifying the effect of metallic coatings on the Kevlar fibers and understanding the yarn pull-out response under high loading rates. Kevlar woven fabrics has demonstrated to perform superior under high loading rates than quasi-static conditions. Further efforts are required to quantify the performance of metallic coated Kevlar fibers and standard Kevlar woven fabrics in high performance ballistic situations.

CHAPTER 3

QUASI STATIC YARN PULL-OUT EXPERIMENTS

This chapter presents a method for characterizing the frictional coefficients of uncoated and coated Kevlar specimens in quasi-static pull-out experiments. Kevlar fabric and hand-woven specimens are tested in a custom-designed fixture at a displacement rate of 1 mm/s and compared through the force displacement response as well as the calculated frictional coefficient and energy absorption.

3.1 METHODS

This approach studies commercially available Kevlar® KM2+ individual yarns are coated with metal layers (copper, aluminum, aluminum nitride, silver) via a directed vapor deposition process. The metal-coated yarns are then hand-woven into fabric swatches. A customized yarn pull-out fixture like the one reported in Zhu et al. [18] is fabricated and is used to investigate the influence of metallic coatings on the quasi-static yarn pull-out behavior. Furthermore, tensile testing is performed to characterize the tenacity, modulus, and failure strain of the yarn for all the coated groups.

3.1.1 Manufacturing metal-coated yarns via directed vapor deposition

Metal-coated Kevlar® yarns are created in this work by applying continuous metal films via a gas jet assisted vapor deposition technique. This approach, shown schematically in Figure 3.1, termed Directed Vapor Deposition (DVD), is based on electron beam evaporation in the presence of an inert carrier gas (see reference [12] for

details). Using the DVD process, metal layers (copper, aluminum, aluminum nitride, silver) are applied onto continuous lengths of 600 denier Kevlar® KM2+ yarns. Prior to coating, a warm water scour is conducted. The yarns are scoured using a package dyeing process. The machine was filled at 49 ℃ and heated to 71 ℃for 20 min, then a drain and rinse step of 5 min at 49 ℃. In package dyeing, the yarn is wound on a small, perforated spool. Studies found that ceramic rollers were best for the least damage to the yarns, and most uniform coatings on the yarns. The winding parameters are set to promote a looser and more open yarn configuration than typical. The spools are placed into the dyeing machine in which the flow of the dye bath alternates from the center to the outside, and then from the outside to the center of the package. This process infiltrates the entire length of yarn on the spool with the dye. The process was repeated 8 times for ideal results. The fluid temperature and the pressure used drive the flow of the dye bath and can be used to control the infiltration process.

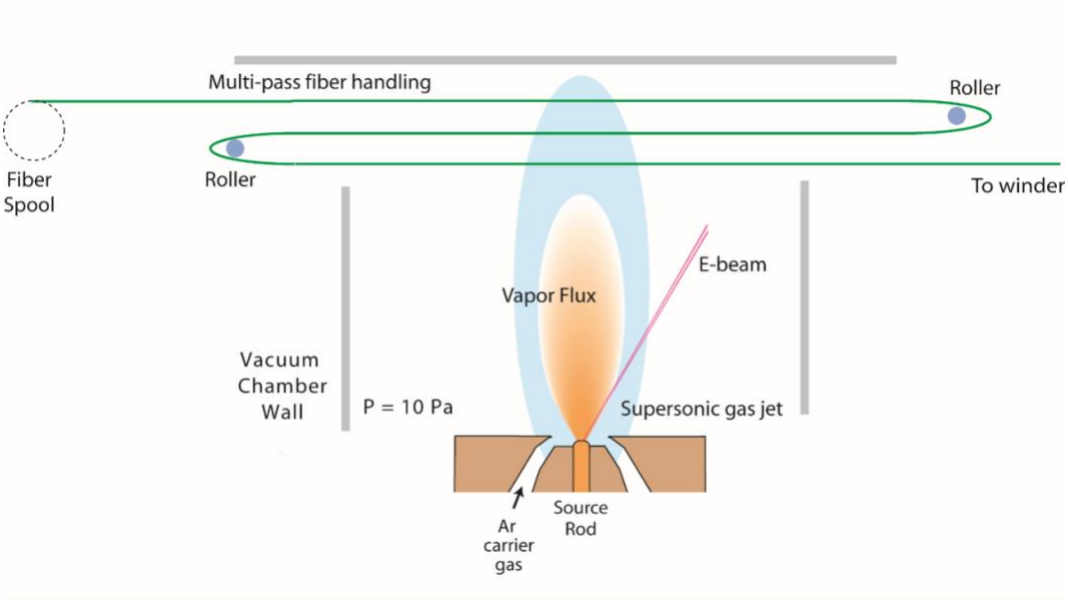

Figure 3.1 Schematic illustration of the Directed Vapor Deposition (DVD) system having a multi-pass yarn handling system

The yarns are fed into and out of the deposition zone with a roll-to-roll yarn handling system. This system allowed the yarns to pass through the deposition zone multiple times at a chosen line speed (up to 91.44 m/min). The coating material was evaporated using an electron beam gun and entrained in an Argon carrier gas. A chamber pressure of 10 Pa is used during deposition. The resulting layers are hypothesized to modify the friction coefficient of the yarn. Denier measurements (see Table 3.1) of the yarn are made by cutting 1-meter-long section of the yarn and measuring the mass in a balance with 0.1 mg resolution. A marginal increase in the denier is measured for the coated groups with a maximum increase of 7.6% for the silver coating. The resulting metal-coated yarns are then hand-woven into fabrics using an aluminum loom with stainless steel pins. Test fabric swatches are created consisting of 34 warp yarns and 50 weft yarns with nominal dimensions of 101.6 mm x 25.4 mm as shown in Figure 3.2.

Figure 3.2 Hand-woven fabric swatches (a) Control (b) Aluminum (c) Hybrid Al/Control (d) Aluminum/Aluminum Nitride (e) Silver (f) Copper

Table 3.1. Coated and uncoated experimental group

Experimental Group	Description	Linear Density (Denier)	Effective fiber diameter (μm)
Control	Warm water rinsed 600 denier Kevlar KM2+	600	12.0
Aluminum	Aluminum Coating on Control	605	12.05
Copper	Copper Coating on Control	637	12.36
Silver	Silver Coating on Control	646	12.45
Aluminum/ Aluminum Nitride	Aluminum/ Aluminum Nitride Coating on Control	627	12.27
Hybrid Al/Control	Hybrid Aluminum (warp)/ Control (weft)	604	12.04
As received	600 denier KM2+ 34X34 Scoured Fabric Roll	600	12.0

Table 3.1 shows the various coated groups studied in this work. The "Control" material is 180 g/m^2, 600 denier sized Kevlar® KM2+ yarn rinsed with warm water. "As-received" is the Kevlar® S706 scoured plain-woven fabric with 600 denier KM2+ yarns, with a fabric count of 34 x 34 yarns per inch in warp and weft directions. Each yarn consists of 400 fibers with a nominal diameter of 12.0 μm. As shown in Figure 3.2, the coated groups include coatings of Aluminum, Copper, Silver, Aluminum/Aluminum Nitride, and a Hybrid Aluminum (warp)/Control (weft). The effective fiber diameter is calculated based on the measured denier and the number of fibers (400). In the Hybrid specimen, warp yarns are Aluminum coated whereas the weft yarns are uncoated as shown in Figure 3.2(c). It should be noted that the hand-woven specimens are not as tightly woven compared to the as-received S706 fabric (shown later in Figure 3.5(a)).

Infiltration of metal coating within the fibers in a yarn may depend on the process conditions such as pass count, line tension, coating time, spreading techniques etc. In this

study, an 8-pass ceramic roller is used to improve coating infiltration. Visual examination of fabric and yarn surfaces in Figures 3.3 (a) and (b) shows that the yarns are indeed coated. Furthermore, scanning Electron Microscopy (SEM) of individual single fibers extracted from Control and some metal-coated groups are shown in Figure 3.3. These images confirm the presence of coated material on the fiber surface. As shown in Figure 3.3(d-f), in Al- and Cu-coated fibers, a “bulk” metal layer is observed whereas in Al/AlN-coated fiber, a distribution of metal particle deposition is observed. Studying coating infiltration, while important, is beyond the scope of this paper.

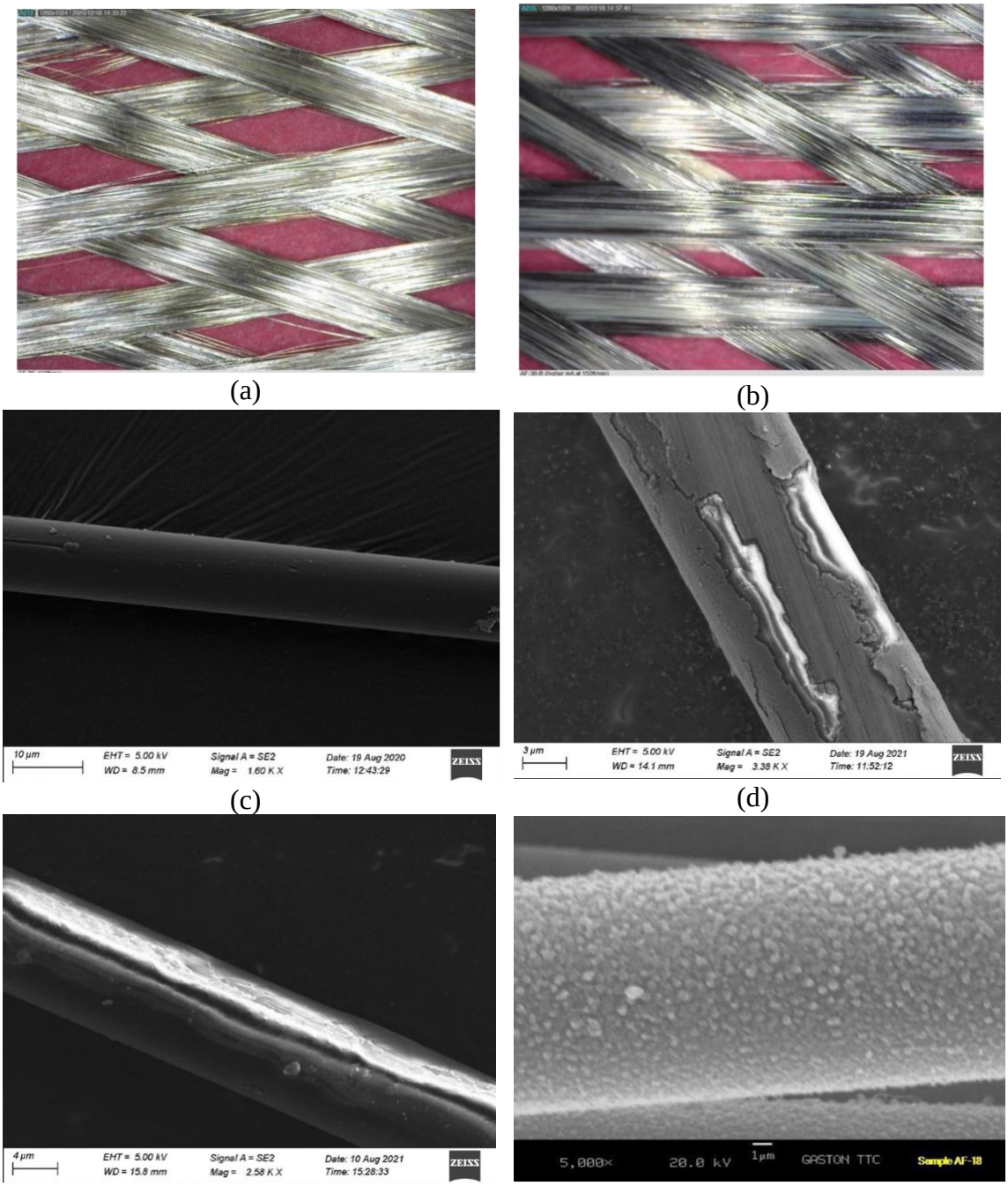

Figure 3.3 (a) Silver-coated yarn (b) Aluminum-coated yarn; SEM images of single fibers (c) Control (d) Aluminum-coated (e) Copper-coated (f) Al/AlN-coated

3.1.2 Quasi-Static yarn pull-out test setup and test methodology

The quasi-static yarn pull-out experimental setup developed in this study utilizing an Instron 5944 machine is shown in Figure 3.4. A custom-designed pull-out fixture is

fabricated using Aluminum 6061.The setup consists of a fixed clamp and a sliding/adjustable clamp with a knurling pattern to clamp the fabric specimen with minimum slippage. The sliding clamp can slide on the railing with carriages and is connected to a screw rod with an adjustable knob to apply various transverse pre-tensions (pre-loads) to the specimen. An Interface SML-450N load cell is used to measure the applied pre-tension. As shown in Figure 3.4, the frame is fixed to the base plate with a X-direction stage to align the yarn to be pulled with the line of action of the Instron's crosshead. A wedge grip attached to a 2 kN load cell is used to pull a single yarn.

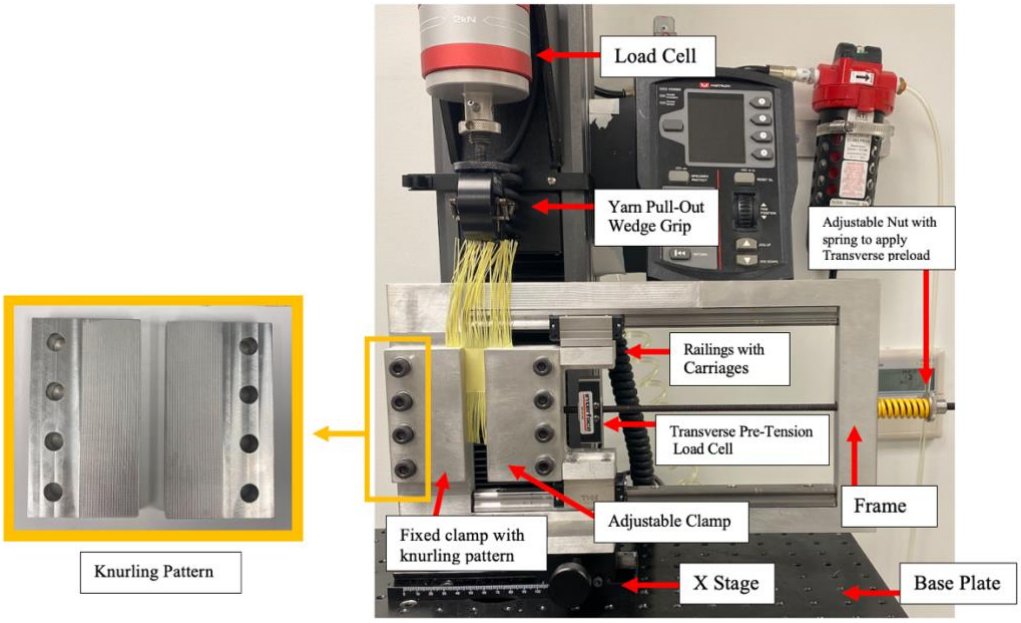

Figure 3.4 Quasi-static yarn pull-out test setup in an Instron machine

Figure 3.5 (a) shows the yarn pull-out specimen with nominal dimensions, the pull pattern used, and the transverse pre-tensions applied. A nominal fabric length of 32 mm and a tail length of 20 mm is used in all experiments. Pull-out tests are performed on a single fabric specimen at three levels (400 N, 200 N, and 100 N) of transverse pre-tension using a pull pattern sequence of 1001001001001001 as shown in Figure 3.5 (a).

Here “1” represents a yarn that is being pulled and “0” represents the adjacent yarn that is skipped. A total of 6 pull-out tests are performed on a single fabric specimen such that 2 tests at each of the three transverse pre-tensions in the order of 400 N, 200 N, and 100 N as shown in Figure 3.5 (a). 1001001 pull pattern is determined based on the repeatability of results after testing multiple pull patterns of different variations. A displacement rate of 1 mm/s is used for all the yarn pull-out experiments. Pull-out force, crosshead pull-out displacement, and transverse pre-tension is recorded. In all the experiments single warp yarns are pulled in the hand-woven fabric specimens. Relaxation tests are performed to confirm that there is no slippage during the pull-out experiments. For the relaxation test, a maximum initial transverse pre-tension of 400 N is applied to the specimen and the transverse load decay is monitored for 120 minutes. As shown in Figure 3.5 (b), the load drop over 120 minutes is less than 1.30%.

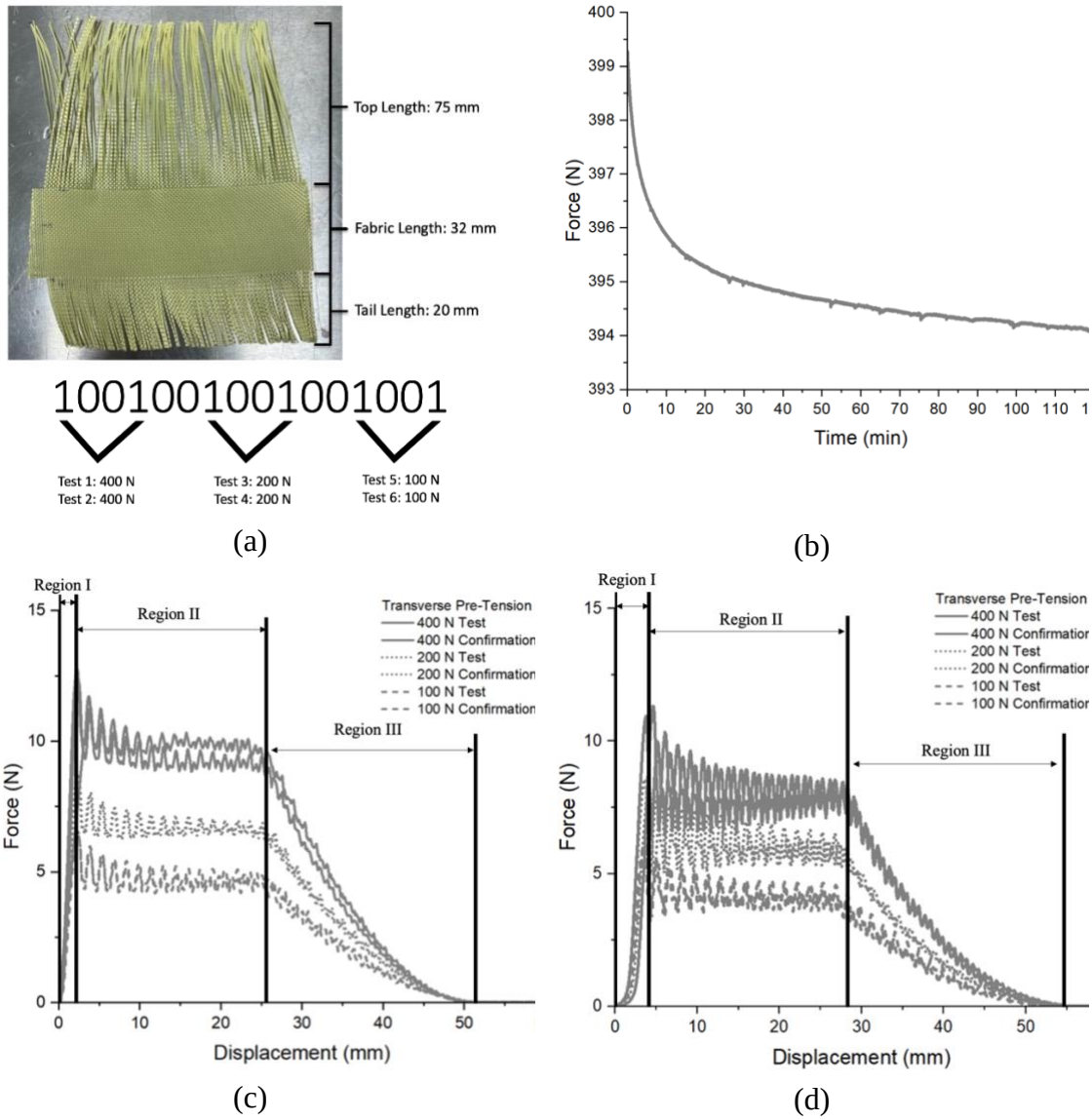

Figure 3.5 (a) Yarn pull-out fabric specimen (b) relaxation response; pull-out force-displacement response of as-received Kevlar S706 fabric with 600 denier KM2+ yarn (c) weft direction (d) warp direction

Preliminary yarn pull-out testing using the as-received Kevlar® S706 fabric is conducted to ensure the experimental results are repeatable and accurate. As shown in Figures 3.5 (c) and 3.5 (d), the yarn pull-out load-displacement response is generally comparable to the results published in the literature [5,19] and is repeatable at different transverse pre-tensions. The pull-out response can be described over three distinct regions. In Region I, the pull-out force increases linearly as the yarn being pulled

undergoes uncrimping and straightening resisted by the static friction of orthogonal yarns in the woven fabric. The end of Region I is characterized by the peak force associated with static friction. Upon reaching the peak force, that is, overcoming the static friction, the pulled yarn begins to slide with a sudden drop in force observed at the beginning of Region II. The oscillations in Region II are due to the stick-slip behavior as the pulled yarn passes through the orthogonal yarns. The length of Region II is approximately equal to the tail length of the specimen. Finally, in Region III, force decreases to zero as the tail length of the yarn traverses through the fabric and gets completely pulled out. The length of the Region III is approximately equal to the length of the fabric.

The integration of pull-out force versus displacement response is used to determine the energy absorbed during the pull-out process for each experimental test. Energy absorption values are divided by the measured tail length and fabric length of each specimen, to allow for consistent results due to the variations in dimensions of the hand-woven specimens.

3.1.2 Quasi-Static yarn tensile setup

Yarns of 254 mm gage length (L_0) from all the experimental groups shown in Table 3.1 are pulled in quasi-static tension according to the ASTM standard D7269-07 [20]. All experiments are performed on an Instron single column tester, Model 5944. A 2 kN load cell and a rate of 127 mm/min is used to test all yarns. Pneumatic Instron grips are used to grip the specimen as shown in Figure 3.6. For each experimental group, at least 25 specimens are tested.

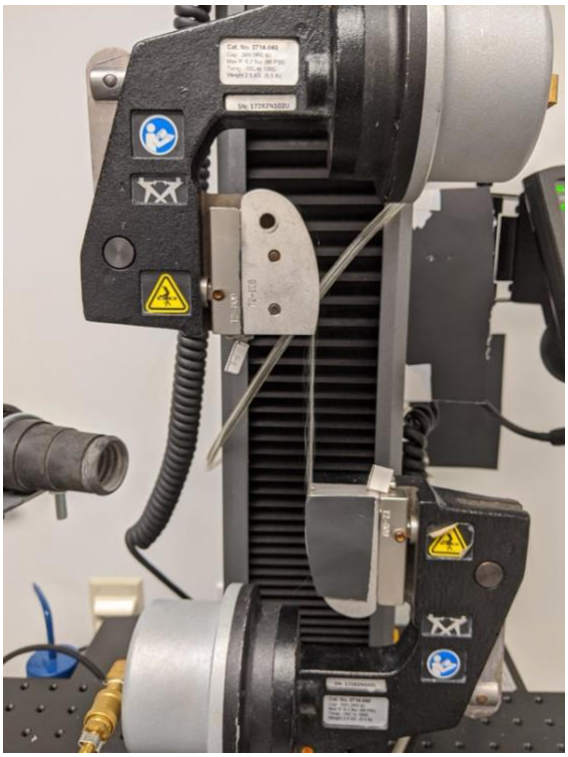

Figure 3.6 Yarn tensile testing experimental setup

The force-displacement measurements from the tensile tests are used to calculate the tenacity versus strain curves using Equation 1.

$$T = \frac{F}{\lambda} \quad \varepsilon = \frac{\Delta L}{L_0} \tag{1}$$

where T is the tenacity, F is the force, and λ is the linear density in denier (see Table 3.1); ε is strain, L_0 is the original gage length, and ΔL is the change in length.

3.2 RESULTS AND DISCUSSION

3.2.1 Yarn pull-out response of hand-woven specimens

Figure 3.7 is the pull-out response of As-received fabric material overlapped with the response of the hand-woven Kevlar. Figure 3.7 shows the As-received material performed approximately 4 times higher than the Control hand-woven specimens.

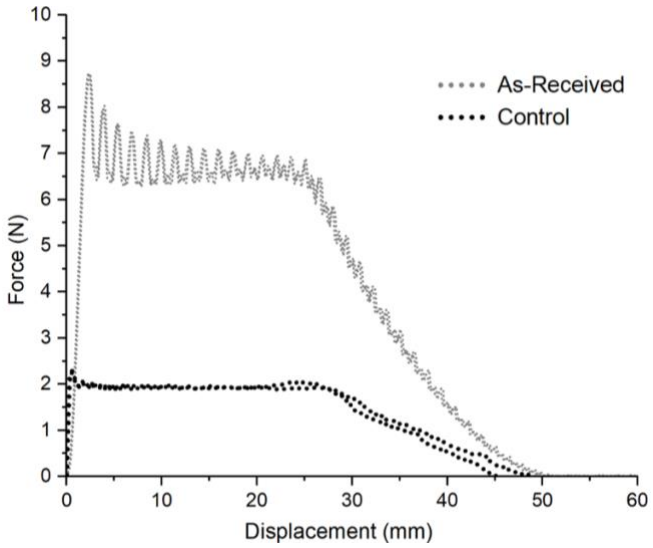

Figure 3.7 Yarn pull-out force-displacement response of 200 N Transverse Pre-Tension control and As-received specimens

Figure 3.8 shows the pull-out process of the hand-woven specimens during the experiments at a transverse pre-load of 400 N. Specifically, Figure 3.8 shows the regions before yarn sliding, during yarn sliding, and complete yarn pull-out for Control, Aluminum/ Aluminum Nitride, and Hybrid Al/Control groups. As the yarn pull-out test is initiated, the yarn undergoes an uncrimping process. The uncrimping process is defined as the straightening of the yarn inside the woven fabric. After the yarn is fully uncrimped, it undergoes translation/sliding until it is completed pulled out from the fabric. The pre-tension applied on the fabric increases the force needed to uncrimp and begin the pull-out process. Unlike control, a high-pitched noise is observed for the metal-coated fabrics during yarn sliding thought to be due to the metal-on-metal contact. Figure 3.8 is showing the pull-out tests are similar during each stage despite coated or uncoated groups, but the frictional coefficients differ between coated and uncoated groups. To determine the discrepancies in fractional coefficients of coated and uncoated groups a further surface.

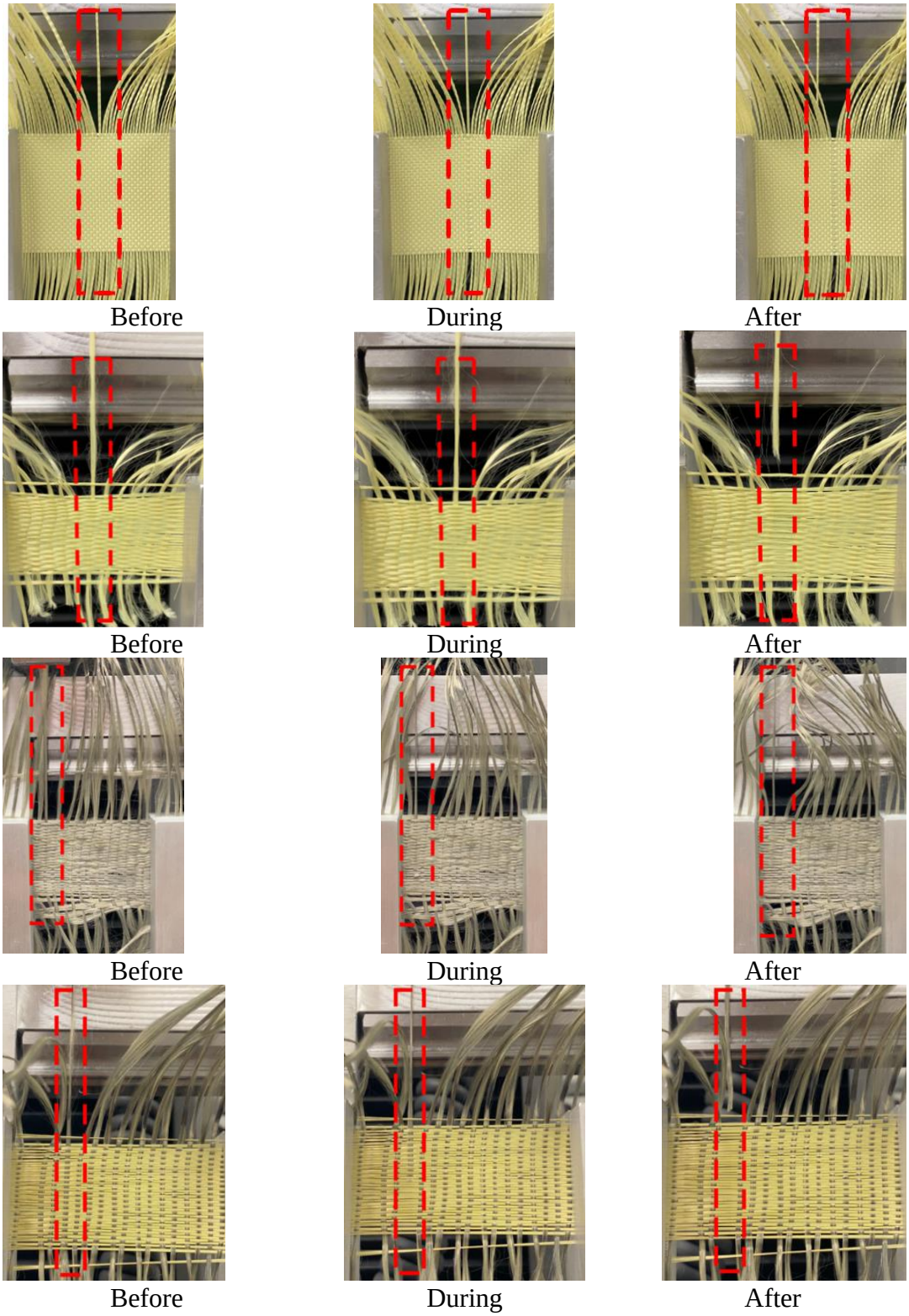

Figure 3.8 Pull-out process at 400 N transverse pre-tension with pulled yarn highlighted in a box (a) Fabric roll S706 (b) Control (c) Al/AlN (d) Hybrid Al/Control

Figure 3.9 shows the yarn pull-out force-displacement response of hand-woven control and metal-coated specimens. The general response of hand-woven specimens are similar to the as-received Kevlar® S706 fabric with three distinct regions (see Figure 3.2 (c)). However, the stick-slip oscillation behavior in Region II is less pronounced, likely due to the "looseness" of the hand-woven weave compared to the as-received S706 fabric. The peak pull-out force in Region I is observed to increase with increase in the transverse pre-tension for all the groups (quantified later). This is likely due to an increase in the normal force between the orthogonal yarns, which also increases the frictional resistance to yarn pull-out [18]. All the metal-coated groups exhibit a higher peak pull-out force and an increased pull-out energy absorption compared to the control at all the transverse pre-tensions studied (quantified later). Upon reaching the peak force, the force drop is sudden and minimal, with the force in Region II (yarn sliding) is approximately constant in control (Figure 3.9 (a)) at all the transverse pre-tensions studied. However, for the metal-coated groups, the force drop is more gradual and the force in Region II is approximately constant at 100 N and 200 N transverse pre-tension. At 400 N pre-tension, the force in Region II continuously decreases with displacement. This suggests that yarn sliding occurs non-uniformly in metal-coated specimens, due to increased frictional sliding resistance and/or variability in coating infiltration, compared to a more uniform yarn sliding in the control specimen. It should be noted that the magnitudes of peak pull-out forces in hand-woven control is approximately 2.5 times lower than the peak forces measured in as-received fabric (see Figure 3.5 (d)).

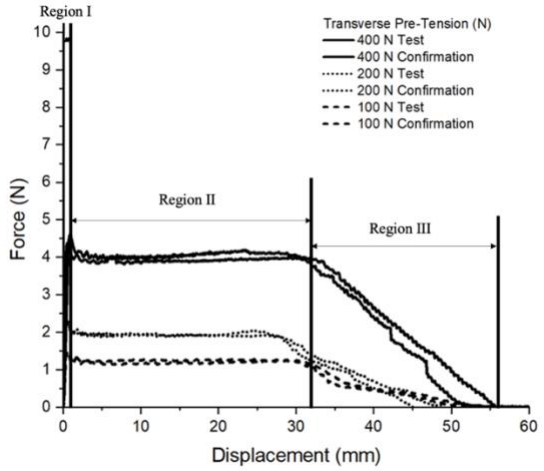

(a) Control

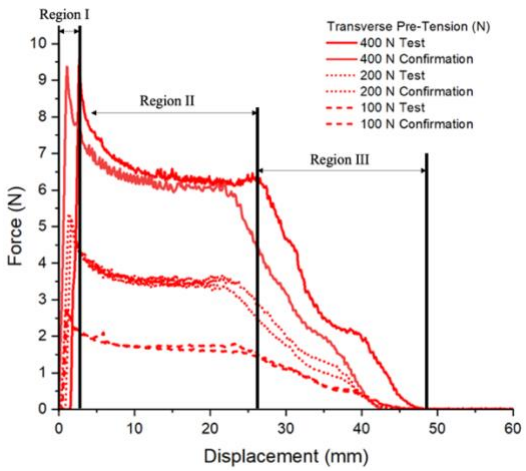

(b) Aluminum

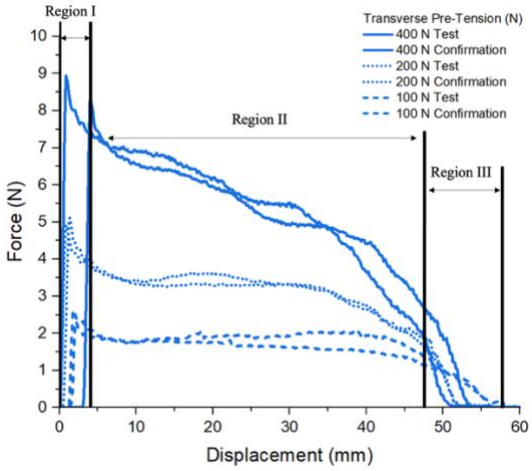

(c) Copper

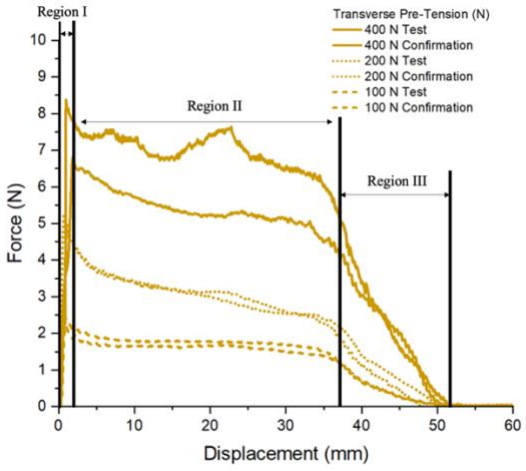

(d) Silver

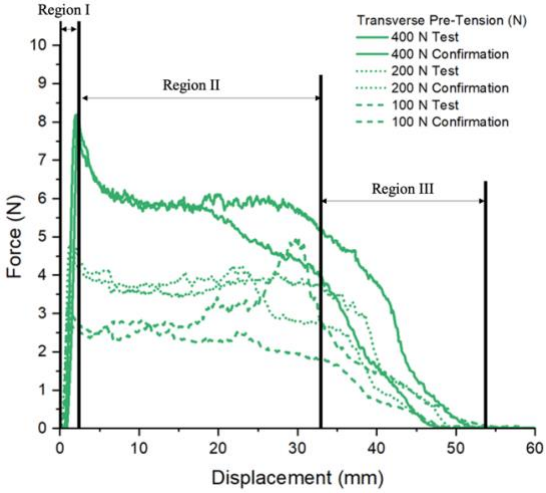

(e) Al/AlN

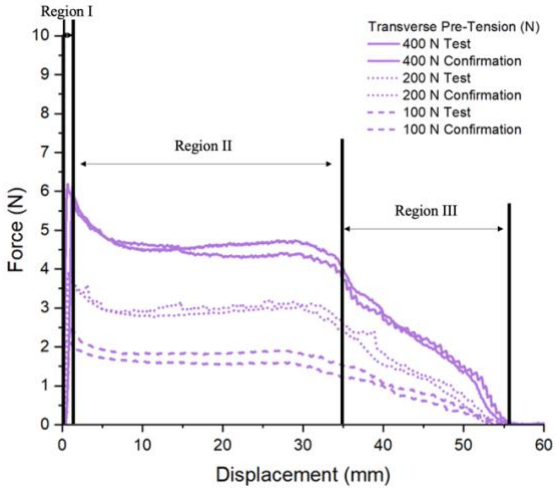

(f) Hybrid Al/Control

Figure 3.9 Yarn pull-out force-displacement response of control and metal-coated groups

As shown in Figure 3.10 (a), the peak pull-out force for all the metal-coated groups is higher than the control at all the three transverse pre-tensions studied. The peak pull-out force increases with increase in transverse pre-tension for all the groups. Furthermore, the rate of increase in the pull-out force with respect to the transverse pre-tension is higher for all the metal-coated specimens than the control. For example, the peak pull-out force increases by a factor of ~3.5 for Aluminum compared to an increase of ~3 for control, going from 100 N to 400 N. The peak pull-out forces are normalized with respect to the corresponding control values and shown in Figure 3.10 (b). Clearly, all the metal-coated groups exhibit an increase in the peak pull-out force compared to the control.

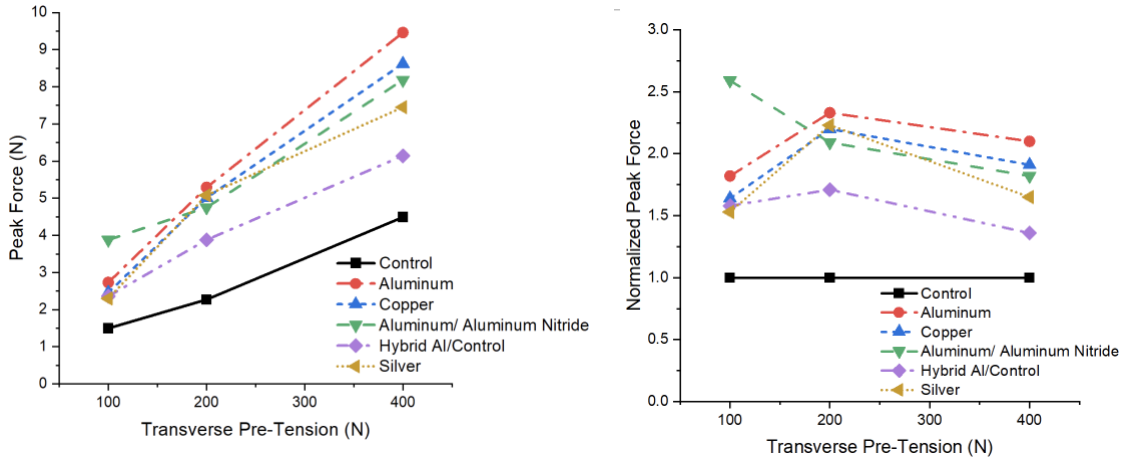

(a) (b)

Figure 3.10 Effect of transverse pre-tension on (a) peak pull-out force (b) normalized peak force

Figure 3.11 shows peak pull-out force and normalized peak pull-out force, as a function of different metal coatings, at a transverse pre-tension of 200 N. All the metal-coated groups except the Hybrid show an increase in the peak pull-out force by a factor

of ~2 compared to the control. The Aluminum-coated specimen shows the highest normalized pull-out force among all the metal-coated groups and has approximately twice the peak pull-out force compared to control. On the other hand, the Hybrid Al/Control specimen shows the lowest normalized peak pull-out force among all the metal-coated groups and has approximately 1.5 times the peak pull-out force compared to control. As discussed before, since peak pull-out force in Region I is associated with static friction, these results suggest that all the metal-coated groups exhibit a significantly enhanced static frictional resistance (behavior) compared to the control.

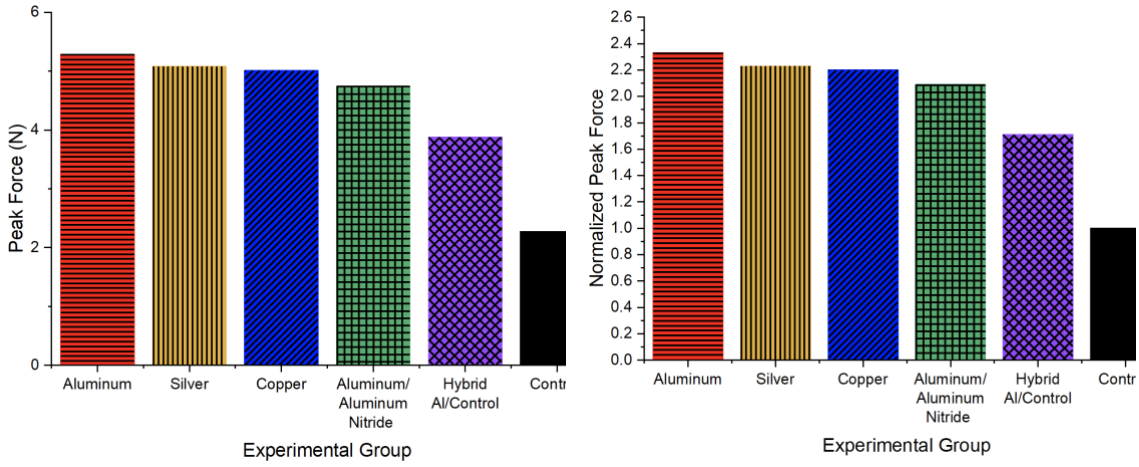

(a) (b)

Figure 3.11 Peak pull-out at 200 N transverse pre-tension (a) peak force (b) normalized peak pull-out force with respect to control

The energy absorbed during the pull-out process due to uncrimping and yarn sliding at various transverse pre-tensions is show in Figure 3.12 (a). Similar to the peak pull-out force, energy absorbed also increases with increase in transverse pre-tension for all the groups studied. Normalized pull-out energy absorption with respect to the corresponding control values are shown in Figure 3.12 (b). All the metal-coated groups exhibit an increase in energy absorption compared to the control.

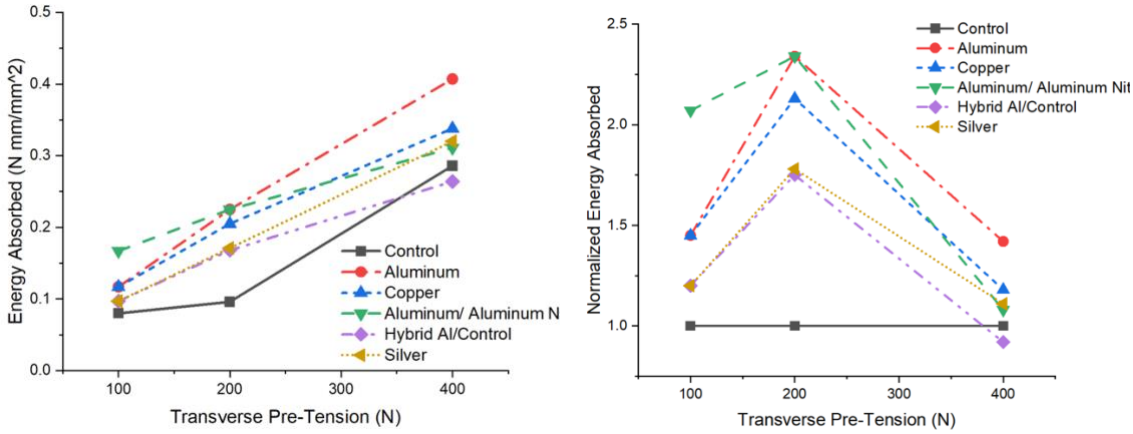

(a) (b)

Figure 3.12 Effect of transverse pre-tension on (a) energy absorbed (b) normalized energy absorbed

Figure 3.13 shows energy absorbed, and normalized energy absorbed, as a function of different metal coatings, at a transverse pre-tension of 200 N. Aluminum specimen shows the highest increase in energy absorption by a factor of ~2.3 compared to the control. Silver and Hybrid Al/Control shows the lowest energy absorption among the metal-coated groups with an increase of ~1.8 compared to control.

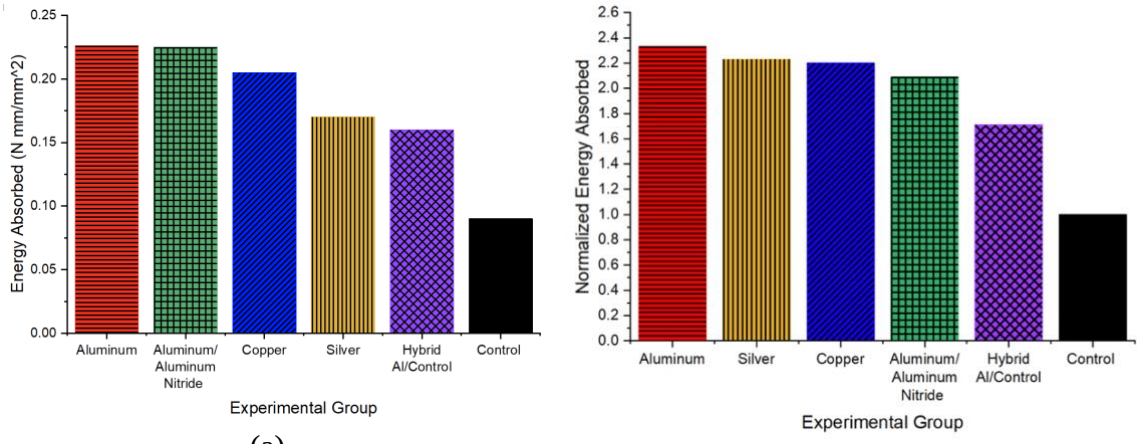

(a) (b)

Figure 3.13 Energy absorbed at 200 N transverse pre-tension (a) energy absorbed (b) normalized energy absorbed with respect to control

The peak pull-out force depends on the fabric architecture and the friction coefficient between the warp and weft yarns among other factors. An empirical relation

for the pull-out force proposed in [4] is given in Equation 2. Here F is the normalized yarn pull-out force per unit fabric length, count is the fabric count in yarns per inch, Diameter is the measured fiber diameter in meters, Modulus is the fiber modulus in Pascal, Waviness is the yarn waviness in meters, Friction indicates the coefficient of cross-yarn friction, and C=0.573 is a constant obtained in [4] from fitting yarn pull-out experimental data without any transverse pre-tension for commercial Kevlar fabrics to Equation 2.

$$F = C \times \text{count}^4 \times \text{Diameter}^2 \times \text{Modulus} \times \text{Waviness} \times \text{Friction} \quad (2)$$

We use this Equation 2 to determine the inter-yarn friction coefficients of the hand-woven fabrics studied in this work. It should be noted that this Equation 2 does not consider the tightness of the weave in the fabric and the effect of transverse pre-tension. Yarn pull-out experiments for the As-received Kevlar® S706 fabric with zero-tail length is first performed without any transverse pre-tension to verify the applicability of Equation 2. Force-displacement response for Kevlar® S706 specimens with a nominal fabric length of 25.4 mm is shown in Figure 3.14. It should be noted that Region II is absent in Figure 3.14 due to the zero-tail length. Using the measured normalized peak pull-out force per unit fabric length and other parameters listed in Table 3.2, a friction coefficient of 0.20 is calculated for the S706 fabric which is comparable to the cross-yarn friction of 0.248 reported in [4] for Kevlar® K706 fabric with KM2 yarns.

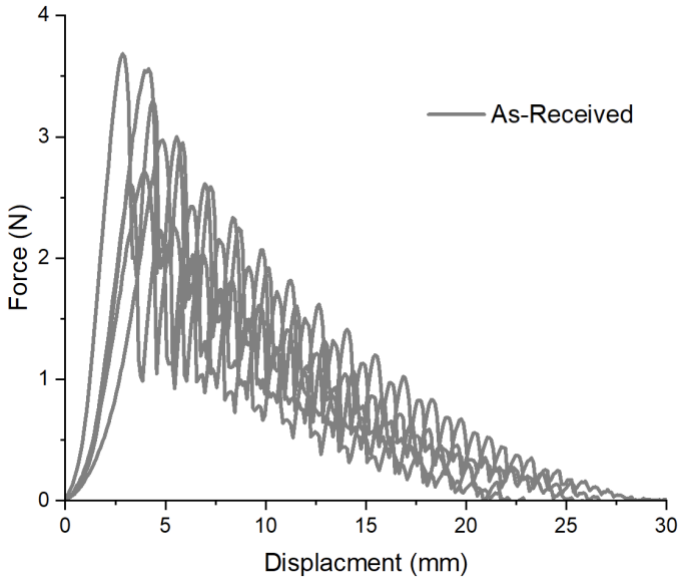

Figure 3.14 Pull-out response of the as-received Kevlar S706 fabric without any transverse pre-tension

Table 3.2 Sample calculations for frictional coefficient using Equation 2

Parameters	Units	As-received Kevlar® S706 without any pre-tension	As-received Kevlar® S706 with 100 N pre-tension	Hand-woven Control with 100 N pre-tension
F	N/m	2.57/0.0254 = 101.18	6.457/0.032 = 201.79	1.495/0.02858=52.3
C	--	0.573	0.573	0.573
Count	Yarns per inch	34	34	50
Diameter	Meter	$1.2\ x\ 10^{-5}$	$1.2\ x\ 10^{-5}$	$1.2\ x\ 10^{-5}$
Modulus	Pascal	$9.2\ x\ 10^{10}$	$9.2\ x\ 10^{10}$	$8.683\ x\ 10^{10}$
Waviness	Meter	$5\ x\ 10^{-5}$	$5\ x\ 10^{-5}$	$5\ x\ 10^{-5}$
Friction		0.20	0.397	0.0233

Since all the hand-woven specimens are tested with non-zero transverse pre-tensions, pull-out force corresponding to 100 N pre-tension is used in all the calculations.

Table 3.2 also lists the parameters used for calculating friction coefficient of hand-woven Control group. A friction coefficient of 0.0233 is calculated for the Control group, which is substantially lower (an order of magnitude) compared to the As-received due to the "looseness" of the weave. Since the hand-woven specimens are not as tightly woven compared to the commercially available Kevlar® fabrics, the friction coefficient values are normalized with respect to the Control values. Furthermore, waviness and fabric count are assumed to be the same for all the hand-woven specimens. Therefore, pull-out force is influenced by the fiber diameter, modulus, and friction coefficient. Knowing the measured fiber diameter (from Table 3.1), measured modulus, and pull-out force per unit fabric length, friction coefficients are calculated for all the groups.

Table 3.3 Normalized frictional coefficients at 100 N transverse pre-tension

Experimental group	Normalized Frictional Coefficient
Control	0.0233/0.0233 = 1
Aluminum	0.0355/0.0233 = 1.52
Copper	0.0407/0.0233 = 1.75
Silver	0.0291/0.0233 = 1.24
Al/AlN	0.0329/0.0233=1.40
Hybrid Al/Control	0.029/0.0233= 1.27

Table 3.3 shows the normalized friction coefficients calculated for all the hand-woven metal-coated groups at a transverse pre-tension of 100 N. All the metal-coated groups show an increase in the normalized friction coefficient compared to the Control. The copper coated specimen shows the highest normalized friction coefficient of 1.75 among all the metal-coated groups. Silver and Hybrid Al/Control shows the lowest normalized coefficient friction of around 1.30. An AFM study to investigate the increase of frictional

coefficients was conducted. The results of surface roughness are found in Table 3.4. A Nanotec WSxM Atomic-Force Microscopy (AFM) is used to investigate the coating of a single fiber that could potentially increase the frictional coefficients. Small piezo tubes measured the as-received S706 and Copper single fibers, whereas a medium piezo tube imaged the Aluminum and Control specimens. Referring to Table 3.4, surface skewness and surface kurtosis values differ for uncoated and coated specimens. Surface skewness is a measurement of the average movement from the symmetry line on the surface. Negative skewness value indicates the surface consists of valleys or cracks, and a positive skewness value contains peaks and asperities. A surface that is negatively skewed is ideal for slippery purposes [21]. From Table 3.4, the Control and As-received S706 experimental groups show negative skewness values as well as the lowest coefficient of friction added with the Hybrid Al/Control studied group. Surface kurtosis is a measurement of sharpness of the asperities. The target value for surface kurtosis is 3 signifying the surface peaks are normally scattered. A surface kurtosis value greater than 3 means the surface has a larger number of peaks and valleys whereas a value lower than 3 is known as the minimal variation in peaks and valleys on a surface [22]. The coated and uncoated groups have a larger variation in surface kurtosis values. The as-received S706 has a value of 3.21 that is close to the target value of 3. The control value is less than 3 which provides knowledge that the surface lacks coatings or damage on the surface. The aluminum and copper coated experimental groups have greater surface kurtosis values which indicates large quantities of particles are present on the yarns. The conclusions of surface skewness and kurtosis values support the calculations of frictional coefficients.

Table 3.4 Atomic-Force Microscope Surface Roughness Comparison Values

	Measured Surface Area (μm^2)	Average Height (nm)	Number of Events	Surface Skewness	Surface Kurtosis
As-Received S706	15.43	23.08	1365	-0.13	3.21
Control	27.41	105.61	1881	-0.31	2.41
Aluminum	27.58	94.577	7500	2.89	25.26
Copper	13.17	25.35	1697	1.74	12.68

Figure 3.15 shows the surface roughness comparison for the measured metallic coatings. The surface roughness of the metallic coatings comparison to the control supported the frictional coefficient increase due to the resistance of sliding of the yarn. The following images in Figure 3.15 provides images for the surface roughness values and displays the changes between the coated and uncoated specimens. The AFM images support the idea that the coating infiltration of the metallic coatings can be studied on a nanometer level.

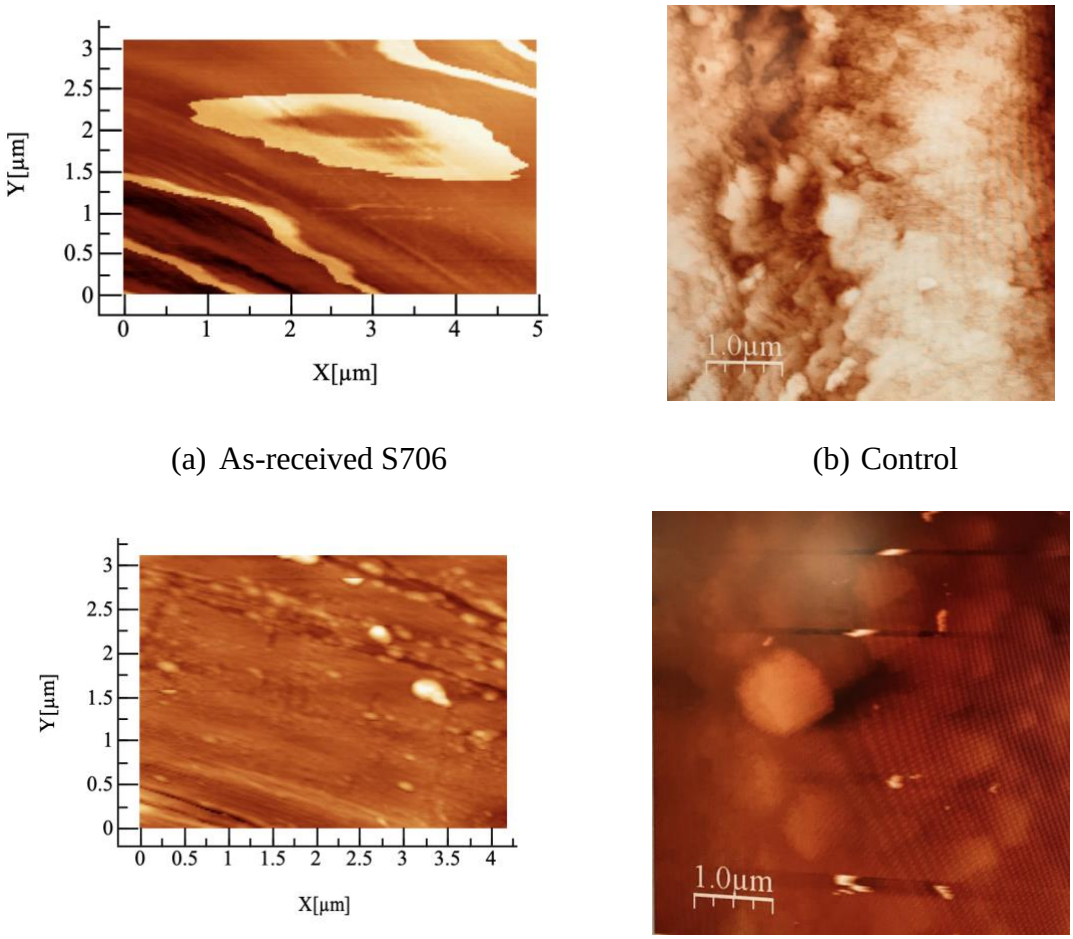

(a) As-received S706 (b) Control

(c) Copper (d) Aluminum

Figure 15. Atomic-Force Microscopy (AFM) surface roughness images of coated and uncoated experimental groups: (a) as-received S706 (b) control (c) Copper (d) Aluminum

Figure 3.16 is a representative graph that shows the comparison for number of events, or particles, to the average height of each particle experienced. As shown in the graph, the aluminum had the largest number of particles, nearly 8 times more than the as-received S706 fabric, as well as the largest average height of the particles. The graph also supports that the metallic coated groups had more particles on a single fiber than the control and as-received S706 fabric.

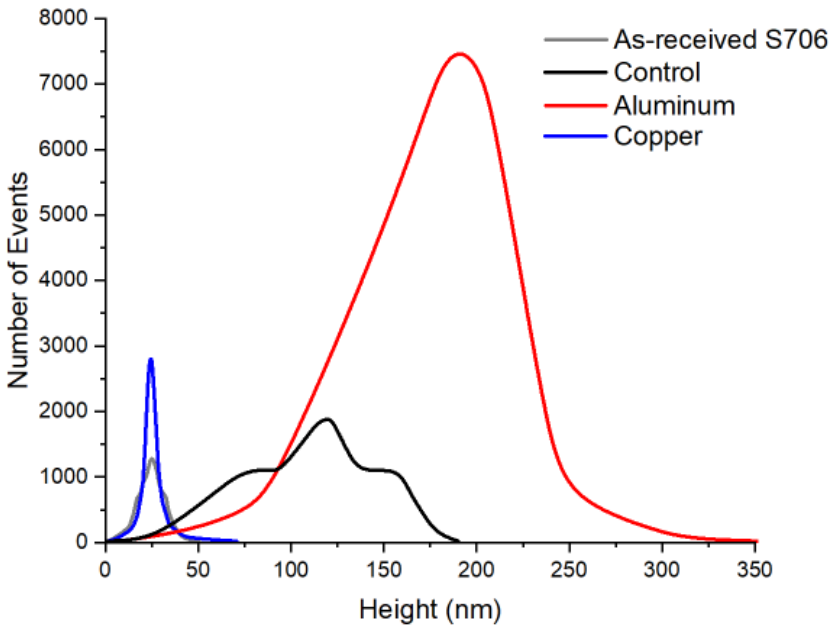

Figure 3.15 Atomic-Force Microscope Surface Roughness Analysis

3.2.2 Tensile testing results

The yarn tensile force-displacement measurements are evaluated in terms of tenacity (force per denier) versus strain. Figure 3.16 (a) shows tensile response of the Control, Figure 3.16 (b) shows the tensile response of the As-received fabric, and Figure 3.16 (c) shows a comparison of the representative tensile response of all the groups. All the groups exhibited an approximately linear response until reaching the peak force. Upon reaching the peak force, a catastrophic failure of the yarn is observed.

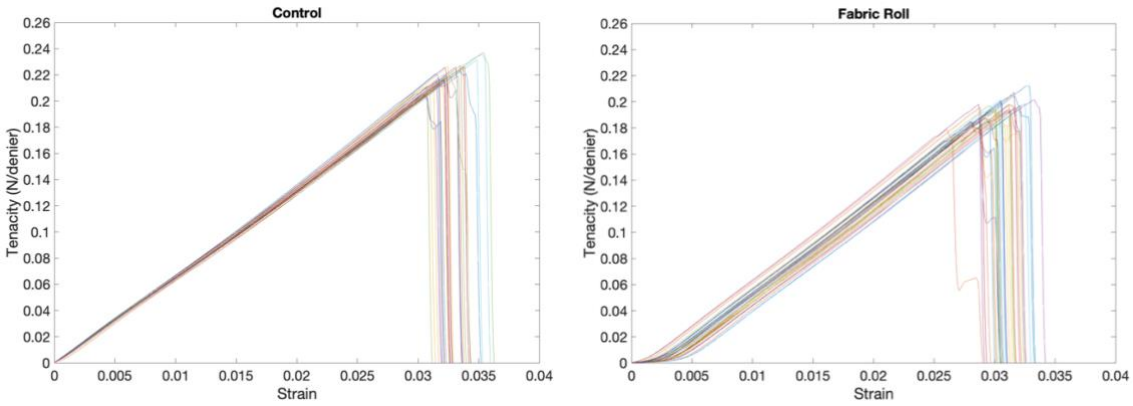

(a)

(b)

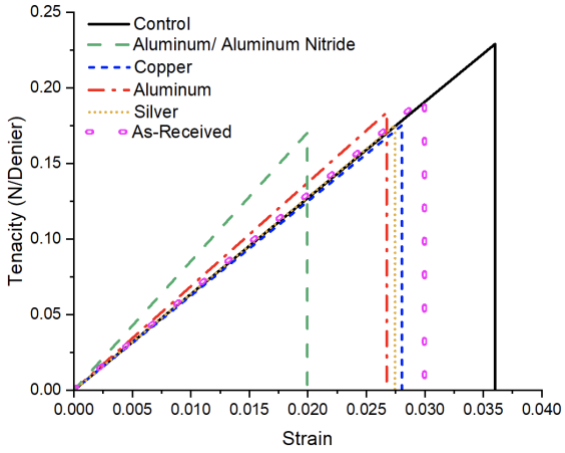

(c)

Figure 3.16 Representative yarn tensile response (a) control yarn tensile response (b) fabric roll S706 (c) representative yarn tensile response of all the groups

Table 3.5 lists the tensile modulus and tenacity measurements for all the groups studied. Differences were determined to be statistically significant ($p<0.05$) by a t-test comparison indicating that the metal-coated groups are significantly different than the control. Tenacity reduction is calculated relative to the control yarn.

Table 3.5. Tensile modulus and tenacity of yarns

Experimental Group	Modulus (GPa)	True tenacity (N/denier)	Percentage reduction in tenacity compared to Control	Strain to failure
Control	86.8 ± 2.4	0.229 ± 0.007	0	0.036 ± 0.001
Aluminum	94.1 ± 1.7	0.1834 ± 0.0058	19.91	0.0267 ± 0.0015
Copper	81.3 ± 2.8	0.1749 ± 0.0096	23.62	0.028 ± 0.001
Silver	89.7± 3.4	0.1757 ± 0.007	23.27	0.0275 ± 0.0018
Aluminum/ Aluminum Nitride	89.1 ± 1.8	0.1706 ± 0.0063	25.50	0.02 ± 0.0007
Hybrid Al/Control	94.0 ± 1.7	0.1834 ± 0.0058	19.91	0.0267 ± 0.0015
As received	92.9 ± 1.1	0.1938 ± 0.007	15.37	0.03 ± 0.0015

In general, the metal-coated yarns showed a marginal increase in the tensile modulus compared to control. However, the metallic coatings resulted in an average of 21.26% reduction in tenacity for all the metal-coated groups compared to control. This is likely due to damage induced to the fibers by the coating process. The metallic coatings add mass to the yarn, increasing the denier of the yarns while not significantly contributing to the tensile strength. Therefore, reducing the tenacity without any real damage to the yarns, but further research is needed to better understand the tenacity reduction mechanisms. As a summary, Figure 3.17 shows the normalized peak pull-out force at 200 N transverse pre-tension and normalized tenacity comparison for all the groups. An increase in the peak pull-out force by a factor of ~ 2 (200%) is accompanied by a decrease in tenacity by ~ 20% compared to control is observed.

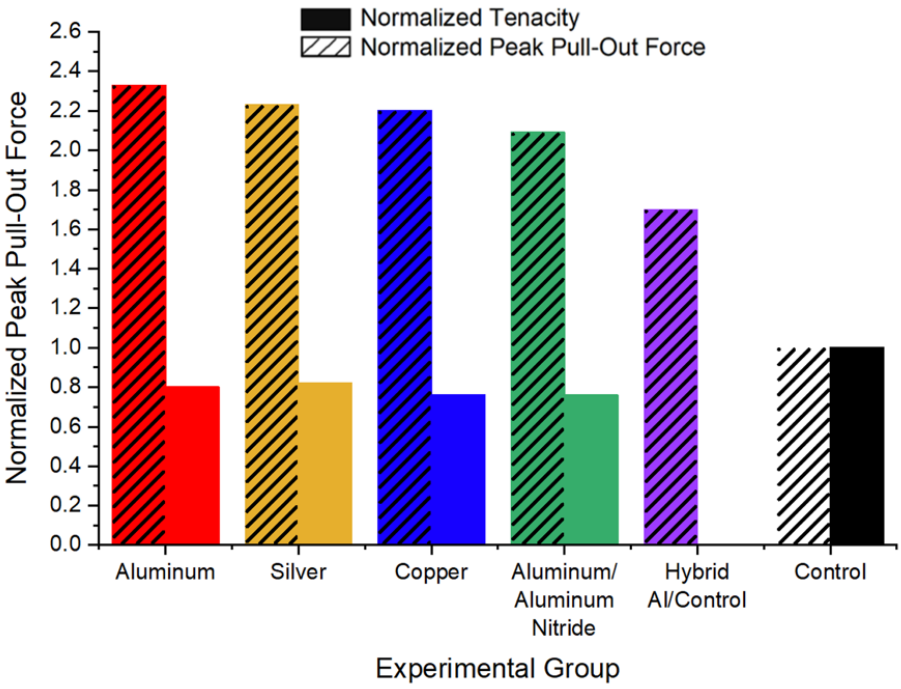

Figure 3.17 Normalized tenacity and peak pull-out tradeoff

3.3 SUMMARY

Experimental studies on the influence of metallic coating on yarn pull-out behavior in Kevlar® fabrics is reported. Kevlar® KM2+ individual yarns are coated with metallic layers (copper, aluminum, aluminum nitride, silver) via a directed vapor deposition process. The uncoated control and metal-coated Kevlar® yarns are hand-woven into fabric swatches. Quasi-static yarn pull-out experiments are performed at three levels of transverse pre-tensions at 100 N, 200 N, and 400 N. Both peak pull-out force and energy absorption during the pull-out process is found to increase with increase in transverse pre-tension. All the metal-coated groups showed an approximately 200% increase in peak pull-out force and a 20% reduction in tenacity compared to uncoated control. Furthermore, all the metal-coated groups showed an increase in energy absorption, with aluminum-coated yarns showing the highest increase of 230% compared

to control. These results suggest enhanced frictional interactions during yarn pull-out in metal-coated yarns compared to uncoated control, but with a tradeoff in reduced tenacity.

CHAPTER 4

DYNAMIC YARN PULL-OUT EXPERIMENTS

This chapter presents a method for dynamic yarn pull-out experiments. A Hopkinson tension bar was changed to accommodate the needs of a yarn pull-out experiment. High velocity cameras and a load cell was used to record force and displacement data and allowed for the test progression to be studied once the test was completed. Frictional Coefficients and energy absorption results were compared to study the response of applied coatings on traditional Kevlar material.

4.1 METHODS

The dynamic method studies Kevlar®S706 woven fabric yarn pull-out response of dynamic loading rates. An experimental woven fabric fixture and single yarn grip fixture was crafted to withstand dynamic loading rates of 15 m/s, 20 m/s, and 25 m/s.

The dynamic yarn pull-out experimental setup was conducted using a Split Hopkinson Pressure Bar setup shown in Figure 4.1. To avoid issues with specimen size discrepancies, the Kistler load cell was attached to a 3-axis positioning stage. A custom yarn grip was threaded to the load cell and clamped the yarn to eliminate any slippage or movement. The woven area of the specimen was placed in a custom maraging 300 steel fixture that threaded into the Split Hopkinson Pressure Bar. It is important to note the fixture threaded into the Split Hopkinson Pressure Bar must be continuous material, with correlating heat treatment, to ensure the wave prorogation was continuous. There were two strain gauges placed on the SHPB testing setup. The first strain

gauge was 1199 mm from the end of the bar, and the second strain gauge was bonded 1268 mm from the end of the bar. The wave speed of the maraging steel was 4870 m/s. The strain gauge was used as a test trigger for all cameras and load cell and used as a secondary tool to confirm the displacement data was accurate. Above the two custom fixtures two Kirana high speed cameras were used to record the response of the L=5 mm and L=27 mm yarns. A Digital Imaging Correlation camera was placed to the side of the fabric fixture to calculate the displacement of the fixture. A pressure velocity study of the pressure chamber was completed prior to testing and was used to reach the target velocities of 15 m/s, 20 m/s, and 25 m/s. A 24" striker bar was determined most useful to achieve the designed testing parameters. The impact gap was set to 5.05 mm to ensure 5 mm minimum pull length was reached for all tests. A copper pulse shaper was used to enhance the response of the strain gauges making the data more accurate. A momentum trap was placed at the end of the experimental test setup to dissipate the velocity of the striker bar, and to stop the striker bar from impacting and ricocheting backwards eliminating the chance to damage the loadcell. The load cell was connected into the displacement camera to eliminate the need to time merging or shifting the data during the analysis.

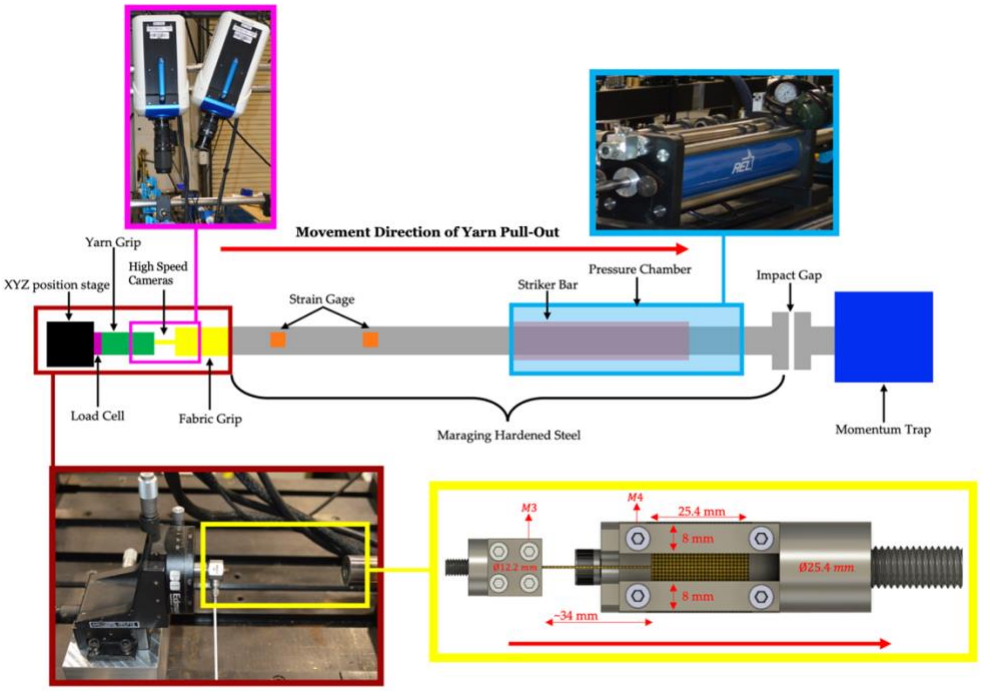

Figure 4.1 Dynamic yarn pull-out tensile Split Hopkinson Pressure Bar experimental schematic and image of setup

Figure 4.2 shows the tested specimens with the denoted difference between a fabric roll L=5 mm specimen and a L=27 mm specimen. The specimen L=5 mm is a 5 mm cut yarn in the woven fabric. The L=27 mm is a non-cut yarn in the woven fabric. Both specimens were tested using the setup shown in Figure 4.1. There are no changes necessary to the experimental setup to test the altered specimens. In Figure 4.2, the image shows an average value for the woven area and top length of the specimen. No tail length was necessary for the designed testing parameters. Three fabric roll S706 specimens shown in Figure 4.2 were tested at each impact velocity of 15 m/s, 20 m/s, and 25 m/s.

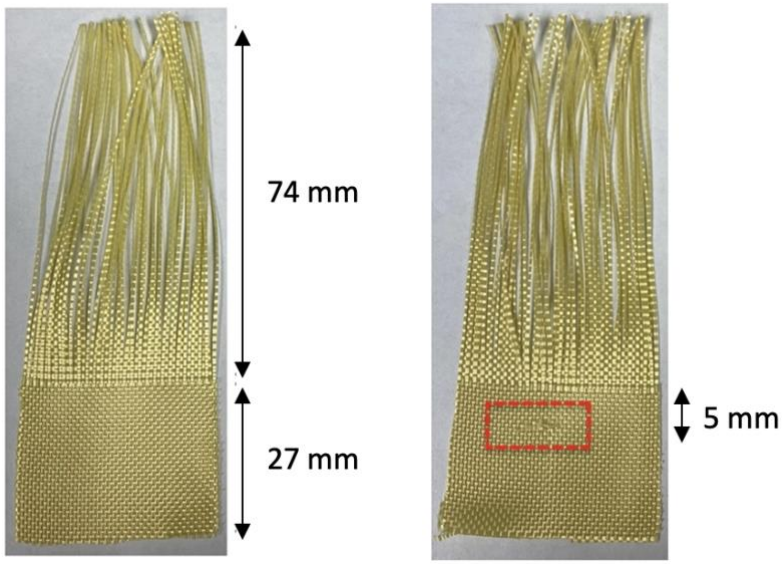

Specimen Length, L=27 mm Specimen Length, L=5 mm

Figure 4.2 Yarn pull-out specimen image with dimensions

The red dotted box is showing where the L=5 mm pull-out yarn is cut on the woven fabric. Figure 4.3 is a representative graph of strain versus time 20 m/s fabric roll S706 test. A 200 μs pretrigger was used to allow data to begin collecting prior to the test. From 0 μs to 200 μs shows the pulse waves traveling through the incident bar. 200 μs to 600 μs is the representative area of the transmitting bar. For the designed test conditions, the reflected pulse data was unnecessary for the data analysis.

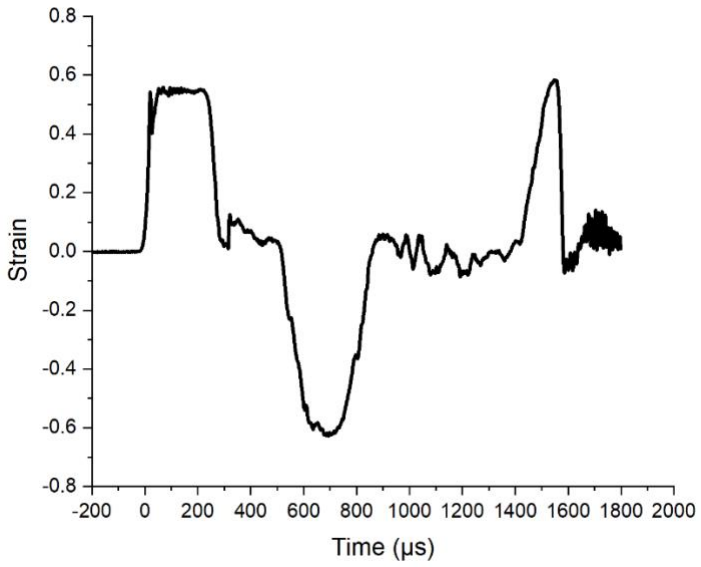

Figure 4.3 Typical strain gage signal, displacement rate of 20 m/s

Figure 4.4 is the graphed results for both Fabric Roll S706 L=5 mm and L=27 mm specimens at 20 m/s loading rate. The force time and displacement time for L=5 mm specimens are shown during the first pulse of the test and includes the start of yarn translation and continues until the yarn is fully pulled from the woven fabric. The Fabric Roll S706 L=27 mm graphs show the full test with the dotted red box noting the area of the 1st pulse. All graphs in Figure 4.4 are representative of 20 m/s displacement rate.

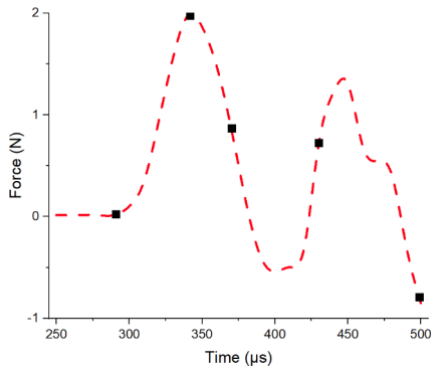

Force-time for L=5 mm, displacement rate of 20 m/s

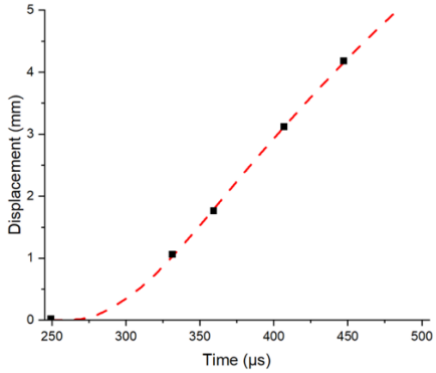

Displacement-time for L=5 mm, displacement rate of 20 m/s

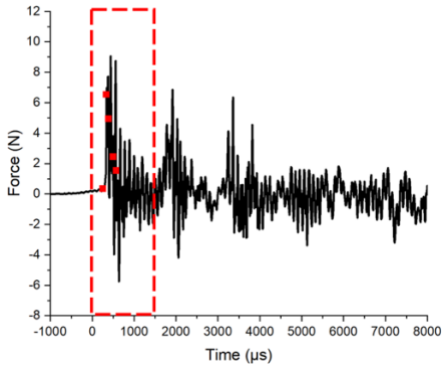

Force-time for L=27 mm full data highlighting 1st pulse, displacement rate of 20 m/s

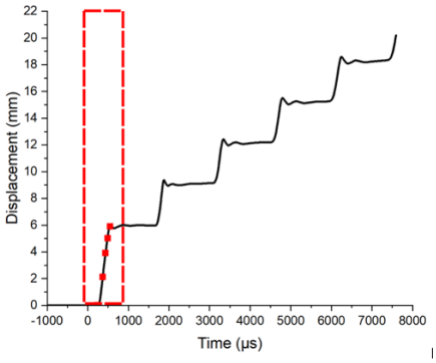

Displacement-time for L=27 mm full data highlighting 1st pulse, displacement rate of 20 m/s

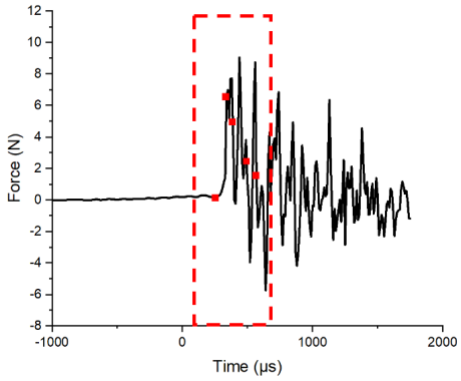

Force-time for L=27 mm continuous tests, displacement rate of 20 m/s

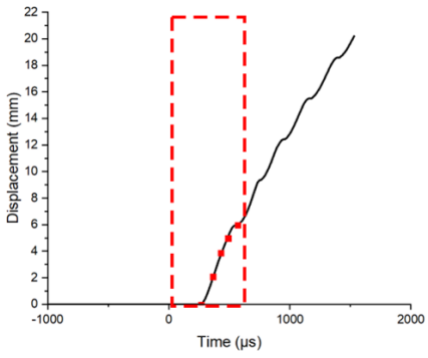

Displacement-time for L=27 mm continuous tests, displacement rate of 20 m/s

Figure 4.4 Representative force-time and displacement-time for as-received Kevlar S706 fabric at a displacement rate of 20 m/s

The shown black dots on the L=5 mm response graphs are the representative peak forces at the labeled time of the sequence images shown in Figure 4.7. The denoted red dots on the L=27 mm graphs are representative of the peak forces of the sequence images shown in Figure 4.8. The time labeled on the sequence images reference the peak forces labeled in Figure 4.4. The integration of pull-out force versus displacement response is used to determine the energy absorbed during the pull-out process for each experimental test. For dynamic tests, Energy absorption values are divided by 5 mm for the L=5 mm tests and divided by the total displacement for the L=27 mm specimens to allow for consistent results due to the variations in the total yarn-pull out length.

4.2 RESULTS AND DISCUSSION

Figure 4.5 is the dynamic pull out response for the L=5 mm and L=27 mm fabric roll S706 specimens specifically studying the response of the 1st pulse. Figure 4.5a is Quasi-static 1 mm/s L=5 mm and L=27 mm results. Figure 4.5b, 4.5c, and 4.5d are the dynamic 15 m/s, 20 m/s, and 25 m/s experimental tests specifically examining the start of yarn translation until the end of the 1st pulse.

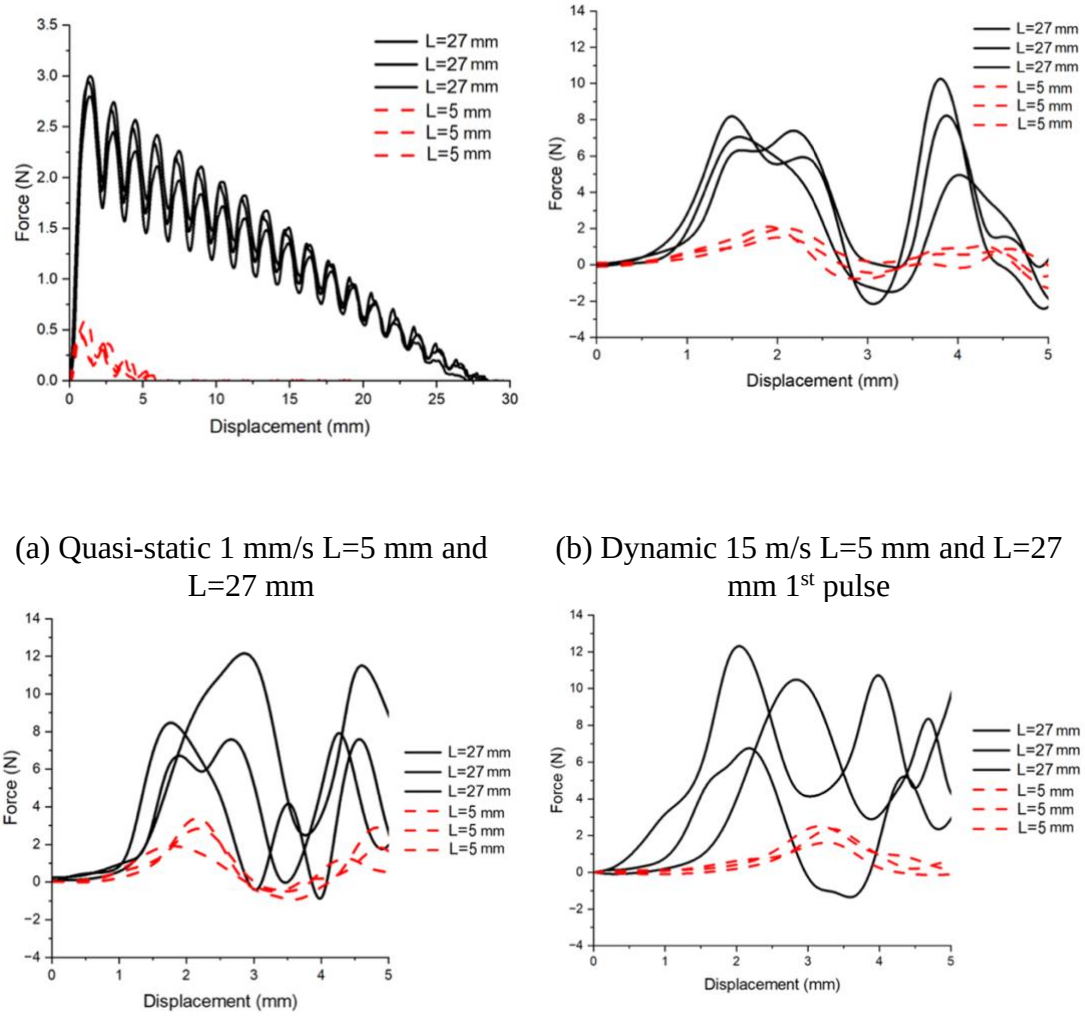

(a) Quasi-static 1 mm/s L=5 mm and L=27 mm

(b) Dynamic 15 m/s L=5 mm and L=27 mm 1st pulse

(c) Dynamic 20 m/s L=5 mm and L=27 mm 1st pulse

(d) Dynamic 25 m/s L=5 mm and L=27 mm 1st pulse

Figure 4.5 Yarn pull-out force-displacement response of as-received Kevlar fabric

Figure 4.6 is a representative graph showing the denoted areas of the yarn-pull out response for prior to the yarn translation, also known as yarn uncrimping, and then the area where the pull-out yarn is undergoing yarn translation. The yarn will experience the uncrimping stage before the translation stage. Once the yarn reaches the translation stage, the yarn will begin to slide through the woven area of the fabric. This schematic is also applied to the calculate energy absorbed values. The yarn uncrimping energy is only calculated in the shown area on Figure 4.6, and the total energy absorbed is the energy of

the yarn uncrimping and yarn translation areas combined to give a value of total energy absorbed.

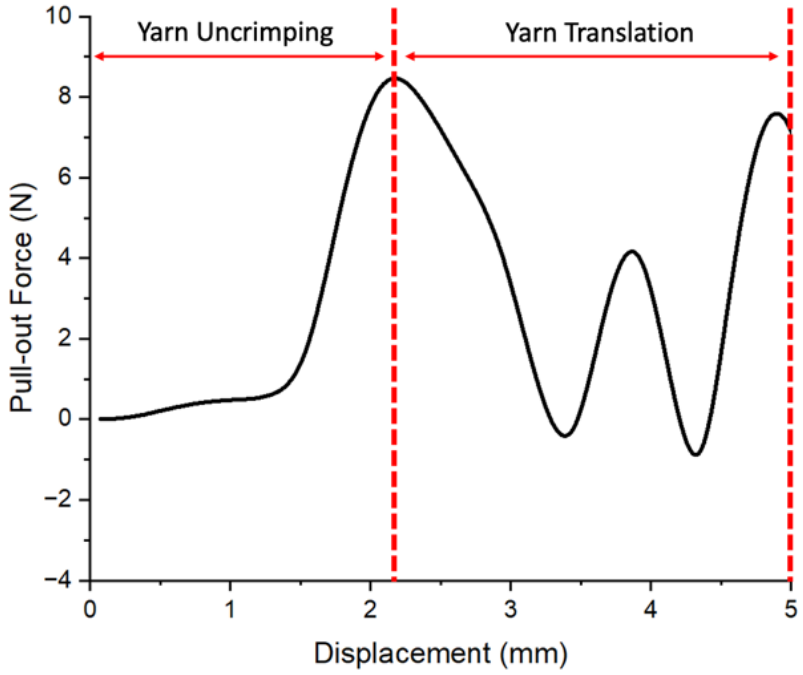

Figure 4.6 Schematic of yarn uncrimping and yarn translation for L=5 mm, 20 m/s displacement rate

Figure 4.7 and Figure 4.8 are pull-out sequence images of a Fabric Roll S706 specimens throughout the phases of the test. Figure 4.7 is the stages an L=5 mm specimen being pulled from the woven fabric. These images show that the yarn is free from the woven fabric once the 1st pulse has been completed. A detail to note about the images in 8a, it provides insight of the placement of the cut yarn inside of the woven fabric. Figure 4.8 is test progression images for a Fabric Roll S706 L=27 mm specimen. The series of images shows the beginning and ending displacement positions of the yarn is approximately 5 mm for the 1st pulse of the test. This conclusion is supported by Figure 4.5. Both image sequence were tested under 20 m/s loading rates.

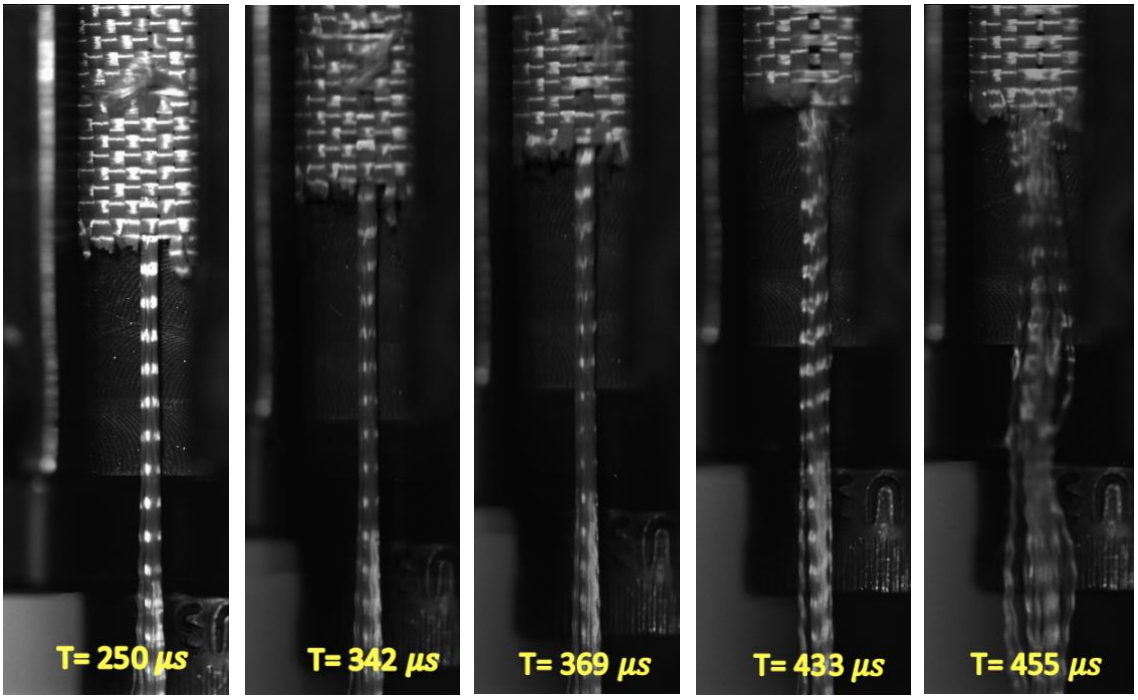

Figure 4.7 Temporal image sequence showing dynamic pull-out process in a L=5 mm specimen, displacement rate of 20 m/s

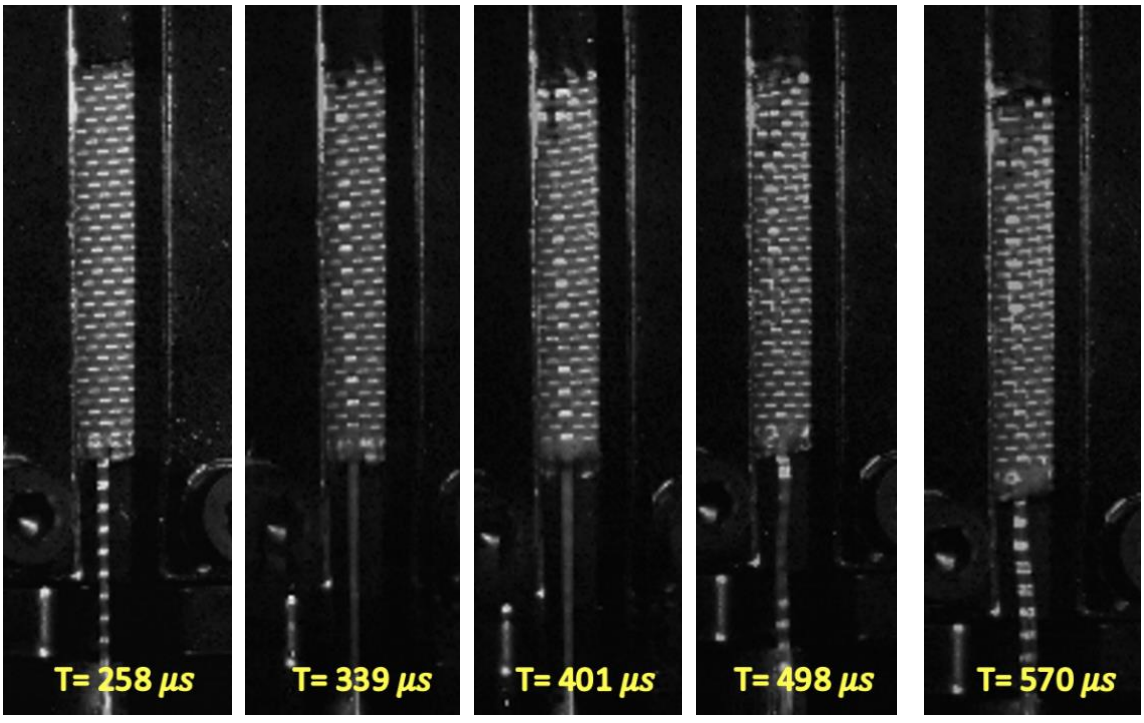

Figure 4.8 Temporal image sequence showing dynamic pull-out process in a L=27 mm specimen, displacement rate of 20 m/s

Figure 4.9a is providing an understanding of displacement rate effects the peak pull-out force for both L=5 mm and L=27 mm fabric roll S706 specimens. Figure 4.9b is an showing the displacement at peak force for each tested dynamic loading rate.

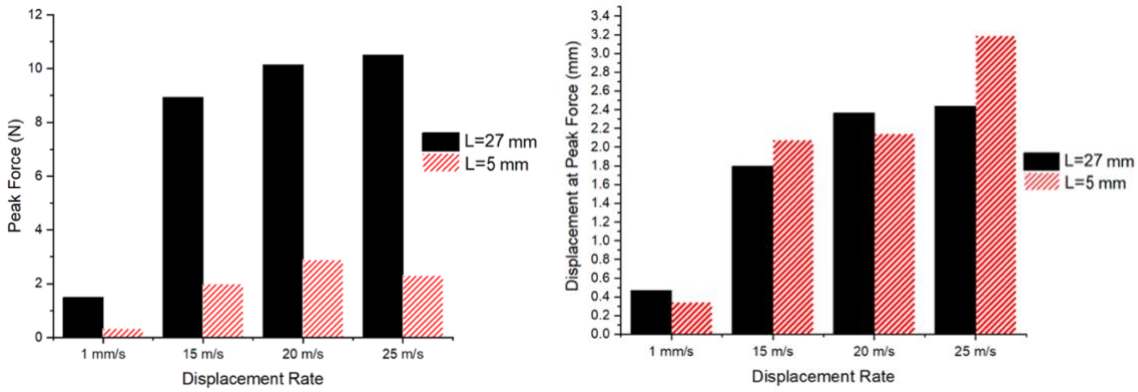

(a) (b)

Figure 4.9 Effect of displacement rate on (a) peak pull-out force (b) displacement at peak force

Figure 4.10a is showing the results for the calculated uncrimping energy which was defined in Figure 4.5 and provides results for all loading rates and L=5 mm and L=27 mm specimens. Figure 4.10b is showing a comparison bar graph for total energy absorbed for the Fabric Roll S706 with all displacement rates and results for L=5 mm and L=27 mm specimens. The uncrimping energy was calculated from the start of the test, removing the pretrigger, until the 1st peak force as represented in Figure 4.6. The total energy was calculated similar as the uncrimping energy except the result of the complete 1st pulse was used. The energy values were calculated using a custom MATLAB script that used a trapezoidal summation rule for calculating the area under the curve.

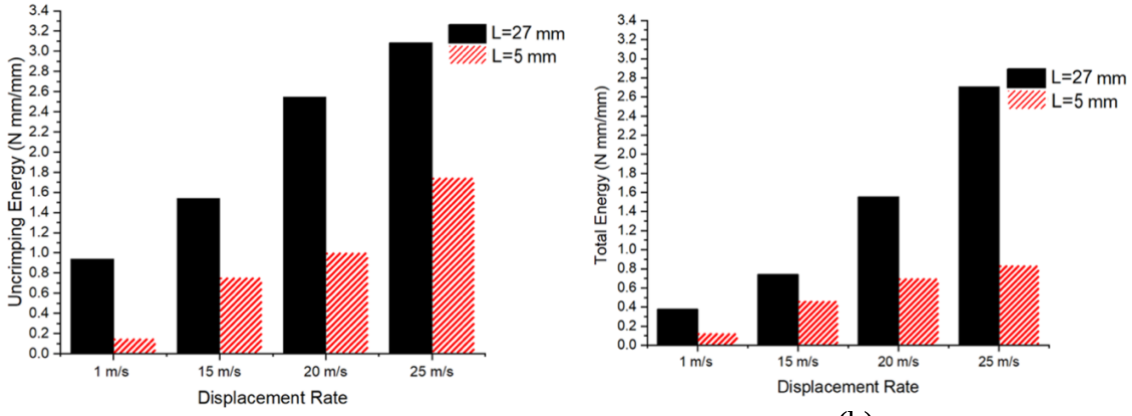

(a) (b)

Figure 4.10 Effect of displacement rate on (a) uncrimping energy (b) total energy absorbed

Figure 4.11 is the comparison of Kevlar specimens with the evaluation of quasi-static to dynamic loading rates. Figure 4.11a is the response of L=27 mm specimens, and Figure 4.11b is the response of L=5 mm specimens and both tests only focusing on the beginning of the test until the 1st pulse. From the graphs in Figure 4.11 the response from quasi-static and dynamic loading rates are similar in response.

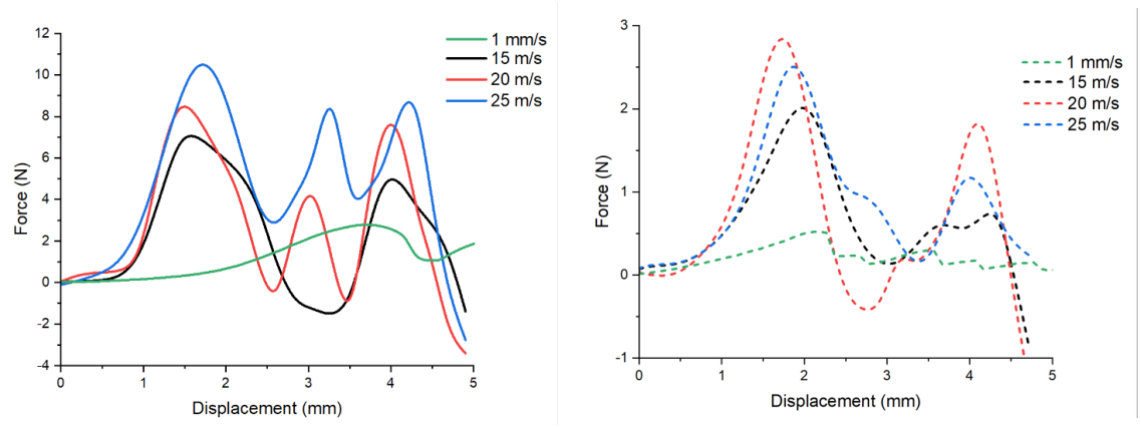

(a) (b)

Figure 4.11 Quasi-static and dynamic yarn pull-out response comparison (a) L=27 mm, first pulse (b) L=5 mm

4.3 SUMMARY

Experimental studies on the influence of dynamic loading rates on yarn pull-out behavior in Kevlar® fabrics is reported. Kevlar® KM2+ woven fabrics are tested under quasi-

static and dynamic loading rates using custom fabricated fixtures. The Quasi-static specimens were tested at 1 mm/s and the dynamic tests were completed at higher loading rate such as 15 m/s, 20 m/s, and 25 m/s. Peak pull-out force and energy absorption increased with increase in loading rates for both L=27 mm and L=5 mm. For the L=27 mm specimens, there was a 33% increase in peak force and approximately 100% increase in energy absorbed with an increase in displacement rates. L=5 mm specimens, there was a 50% increase with an increase from 15 m/s to 20 m/s, but a slight decrease in peak force once reaching 25 m/s. L=5 mm tested specimens energy absorption values shows an 130% increase with an increase in displacement rates. Dynamic loading tests showed higher peak force and energy absorption values than quasi-static experiments. The improved peak force and energy absorption values can be directly correlated to improved ballistic performances. The dynamic experiments are modeled in LS-DYNA using a custom used model. Model predictions correlate well to the experimental observations and allow for the peak force and energy absorbed quantitative values to be accurately compared between experimental and theoretical outputs.

CHAPTER 5

CONCLUSIONS AND FUTURE WORK

In this thesis, a critical review of the existing body of literature concerning dynamic load rates and modified Kevlar fibers has been performance, which details previous efforts to quantify the response of metallic coated Kevlar fibers and understanding the dynamic response of high loading rates on woven fabrics for the purpose of increasing the ballistic impact performance.

One notable experimental procedure which has not been described in literature is yarn dynamic yarn pull out using a Split Hopkinson Pressure Bar. In order to fully meet the needs of material characterization of metallic coated Kevlar and testing woven Kevlar fabrics under dynamic loading rates two apparatuses has been developed. They have been developed on the idea of testing the metallic coated woven Kevlar fabrics under quasi-static yarn pull out, and standard Kevlar S706 fabrics undergoing dynamic loading rates. The metallic coatings consisted of Aluminum, Copper, Silver, and Aluminum/Aluminum Nitrite, and displacement rates of 15 m/s, 20 m/s, and 25 m/s. Using this method, the data has been successfully obtained and correlates well with previous experimental efforts with other configurations. Peak forces and Energy absorbed for both approaches both increased with the applied metallic coatings and increase in dynamic loading rates. For the first approach, there was approximately a 200% increase in peak pull-out force and a 20% reduction in tenacity compared to the uncoated control. All metal coated groups showed an increase in energy absorption, with

aluminum-coated yarns showings the highest increase of 230% compared to the control. The results suggest enhanced frictional interactions during yarn pull-out in metal-coated yarns compared to the uncoated control and is proved by the frictional calculations. The second method showed that for both L=5 mm and L=27 mm there is an increase in peak force and energy absorption values with an increase in displacement rates. The L=27 mm specimens showed a 33% increase in peak force and 110% increase in energy absorbed with an increase in dynamic loading rates. The L=5 mm specimens showed a 50% increase in peak force from 15 m/s to 20 m/s but a slight decrease in peak force when increased to 25 m/s. The energy absorbed for L=5 mm specimens showed an increase of 130% with the increase of displacement rate. All dynamic loading tests showed higher peak forces and energy absorption values than quasi-static experiments. Furthermore, addition improvements could be made to each approach. For the metallic coated Kevlar specimens, it is visible that the coating throughout the Kevlar yarns is not uniform. Applying a uniform coating to the Kevlar yarns before weaving could impact the frictional coefficients and further increase the ability of ballistic performance. The tested specimens were hand-woven, and the tightness of the weave could be improved. Having the baseline knowledge of which coating performed superior and allowing a machine to uniformly weave the metallic coated Kevlar into a fabric would also strengthen the results of the experiments. For the second approach, there were visible issues with the fabric fixture. The intensity of the experiment caused many of the grip bolts to shear and voided the test. Redesigning the fixture to eliminate the grip bolts would eliminate the room for error or slippage during testing as well as eliminating the likelihood of any injuries or damages to the equipment or personnel. The techniques and concepts

developed and applied in this work will be imperative in growing the understanding of Kevlar in ballistic impact performance. The two suggested approaches will be critical in the future advancements of Kevlar applications.

REFERENCES

[1] Sockalingam S, Chowdhury SC, Gillespie JW, Keefe M. Recent advances in modeling and experiments of Kevlar ballistic fibrils, fibers, yarns and flexible woven textile fabrics – a review. Text Res J 2016. https://doi.org/10.1177/0040517516646039.

[2] Cunniff PM. An analysis of the system effects in woven fabrics under ballistic impact. Text Res J 1992;62:495–509.

[3] Gawandi A, Thostenson ET, Gilllespie Jr JW. Tow pullout behavior of polymer-coated Kevlar fabric. J Mater Sci 2011;46:77–89.

[4] Dong Z, Sun CT. Testing and modeling of yarn pull-out in plain woven Kevlar fabrics. Spec Issue CompTest 2008 2009;40:1863–9. https://doi.org/10.1016/j.compositesa.2009.04.019.

[5] Nilakantan G, Gillespie JW. Yarn pull-out behavior of plain woven Kevlar fabrics: Effect of yarn sizing, pullout rate, and fabric pre-tension. Compos Struct 2013;101:215–24. https://doi.org/10.1016/j.compstruct.2013.02.018.

[6] Kirkwood KM, Kirkwood JE, Lee YS, Egres RG, Wagner NJ, Eric D, et al. Yarn Pull-Out as a Mechanism for Dissipating Ballistic Impact Energy in Kevlar® KM-2 Fabric : Part I: Quasi-Static Characterization of Yarn Pull-Out. Text Res J 2004;74:920–8. https://doi.org/10.1177/004051750407401012.

[7] LaBarre ED, Calderon-Colon X, Morris M, Tiffany J, Wetzel E, Merkle A, et al. Effect of a carbon nanotube coating on friction and impact performance of Kevlar.

J Mater Sci 2015:1–12.

[8] Duan Y, Keefe M, Bogetti TA, Cheeseman BA, Powers B. A numerical investigation of the influence of friction on energy absorption by a high-strength fabric subjected to ballistic impact. Int J Impact Eng 2006;32:1299–312.

[9] Decker MJ, Halbach CJ, Nam CH, Wagner NJ, Wetzel ED. Stab resistance of shear thickening fluid (STF)-treated fabrics. Compos Sci Technol 2007;67:565–78.

[10] Dong Z, Manimala JM, Sun CT. Mechanical behavior of silica nanoparticle-impregnated Kevlar fabrics. J Mech Mater Struct 2010;5:529–48.

[11] Tan VBC, Tay TE, Teo WK. Strengthening fabric armour with silica colloidal suspensions. Int J Solids Struct 2005;42:1561–76.

[12] Groves, J.F.;Mattusch, G.;Morgner, H.;Haas, D.D.; Wadley HN. Directed vapour deposition. Surf Eng 2000;16:461–4.

[13] Buckley DH. Friction and wear of tin and tin alloys from 110 to 150 C. NASA Tech. Note D-8004, Washington, DC 1975.

[14] Buckley DH. Friction, wear, and lubrication in vacuum. National Aeronautics and Space Administration 1971.

[15] Rabinowicz E. Friction coefficients of noble metals over a range of loads. Wear 1992;159:89–94.

[16] Antler M. Wear and friction of the platinum metals. Platin Met Rev 1966;10:2–8.

[17] Sockalingam S, Casem D, Weerasooriya T, McDaniel P, Gillespie J. Experimental Investigation of the High Strain Rate Transverse Compression Behavior of Ballistic Single Fibers. J Dyn Behav Mater 2017;3:474–84. https://doi.org/10.1007/s40870-017-0126-2.

[18] Zhu D, Soranakom C, Mobasher B, Rajan SD. Experimental study and modeling of single yarn pull-out behavior of kevlar® 49 fabric. Compos Part A Appl Sci Manuf 2011;42:868–79. https://doi.org/http://dx.doi.org/10.1016/j.compositesa.2011.03.017.

[19] Das S, Jagan S, Shaw A, Pal A. Determination of inter-yarn friction and its effect on ballistic response of para-aramid woven fabric under low velocity impact. Compos Struct 2015;120:129–40. https://doi.org/10.1016/j.compstruct.2014.09.063.

[20] D7269, Standard test methods for tensile testing of aramid yarns 2017.

[21] Kirkwood JE, Kirkwood KM, Lee YS, Egres RG, Wagner NJ, Wetzel ED. Yarn Pull-Out as a Mechanism for Dissipating Ballistic Impact Energy in Kevlar® KM-2 Fabric Part II: Predicting Ballistic Performance. Text Res J 2004;74:939–48.

[22] Kirkwood KM, Kirkwood JE, Lee YS, Egres RG, Wagner NJ, Eric D, et al. Textile Research Journal 2004. https://doi.org/10.1177/004051750407401012.

[23] Guo, Zherui, et al. “Loading Rate Effects on Dynamic out-of-Plane Yarn Pull-Out.” *Textile Research Journal*, vol. 84, no. 16, 2014, pp. 1708–1719., doi:10.1177/0040517514527376.

[24] Yeheskel O. Ultrasonic characterization of aging behavior in M250 grade maraging steel. Metall Mater Trans A Phys Metall Mater Sci 2009;40:684–90. https://doi.org/10.1007/s11661-008-9740-x.

[25] Cheng M, Chen W, Weerasooriya T. Experimental investigation of the transverse mechanical properties of a single Kevlar® KM2 fiber. Int J Solids Struct 2004;41:6215–32. https://doi.org/10.1016/j.ijsolstr.2004.05.016.

[26] Duan Y, Keefe M, Bogetti TA, Cheeseman BA. Modeling friction effects on the ballistic impact behavior of a single-ply high-strength fabric. Int J Impact Eng 2005;31:996–1012. https://doi.org/10.1016/j.ijimpeng.2004.06.008.

[27] Wang Y, Xia Y. The effects of strain rate on the mechanical behaviour of kevlar fibre bundles: An experimental and theoretical study. Compos Part A Appl Sci Manuf 1998;29:1411–5. https://doi.org/10.1016/S1359-835X(98)00038-4.

[28] Cheng M, Chen W, Weerasooriya T. Mechanical properties of Kevlar® KM2 single fiber. J Eng Mater Technol 2005;127:197–203. https://doi.org/10.1115/1.1857937.

[29] Ashvani Goyal 13 - Defense applications of manikins, Editor(s): Rajkishore Nayak, Rajiv Padhye, In Woodhead Publishing Series in Textiles, Manikins for Textile Evaluation, Woodhead Publishing, 2017, Pages 279-300, ISBN 9780081009093, https://doi.org/10.1016/B978-0-08-100909-3.00013-3.

[30] Tanner, D., Fitzgerald, J.A. and Phillips, B.R. (1989), The Kevlar Story—an Advanced Materials Case Study. Angew. Chem. Int. Ed. Engl., 28: 649-654. https://doi.org/10.1002/anie.198906491

[31] An Optical method for measuring surface roughness and machined carbon fibre-reinforced plastic composites. (N Duboust)

[32] https://engineering.purdue.edu/ME556/Documents/Surface%20Roughness.pdf